(19) Europäisches Patentamt
European Patent Office
Office européen des brevets

(11) EP 2 592 627 A1

(12) EUROPEAN PATENT APPLICATION

(43) Date of publication:
15.05.2013 Bulletin 2013/20

(51) Int Cl.:
G21K 1/06 *(2006.01)*

(21) Application number: **11195264.4**

(22) Date of filing: **22.12.2011**

(84) Designated Contracting States:
AL AT BE BG CH CY CZ DE DK EE ES FI FR GB GR HR HU IE IS IT LI LT LU LV MC MK MT NL NO PL PT RO RS SE SI SK SM TR
Designated Extension States:
BA ME

(30) Priority: **08.11.2011 EP 11188251**

(71) Applicants:
- **Ludwig-Maximilians-Universität München**
  80539 München (DE)
- **INSTITUT MAX VON LAUE - PAUL LANGEVIN**
  38042 Grenoble Cedex 9 (FR)
- **Max-Planck-Gesellschaft zur Förderung der Wissenschaften e.V.**
  80539 München (DE)

(72) Inventors:
- **Habs, Dietrich**
  81679 Munich (DE)
- **Günther, Marc**
  64291 Darmstadt (DE)
- **Jentschel, Michael**
  38360 Sassenage (FR)

(74) Representative: **Lucke, Andreas**
Boehmert & Boehmert
Pettenkoferstrasse 20-22
80336 München (DE)

(54) Refractive optics for gamma-photons

(57) The present invention relates to a use of one or more refractive optical elements for shaping, deflecting and/or guiding by total internal reflection a beam of γ-photons having an energy for which the energy dependent index of refraction of the material of said refractive optical element has a real part that is larger than 1.

Fig. 9

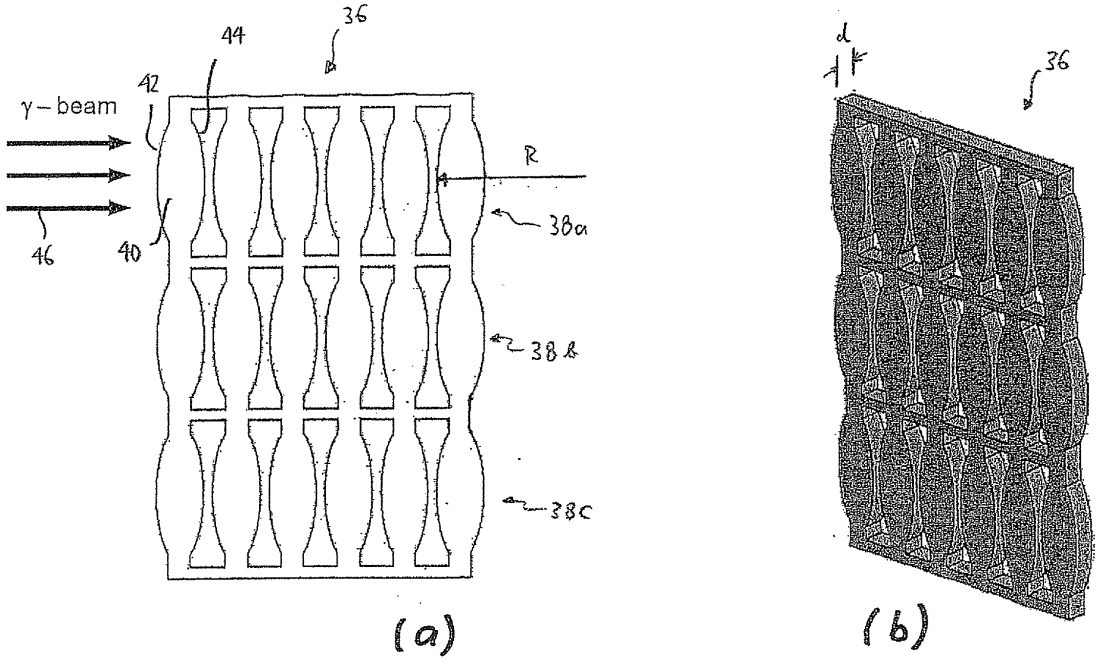

EP 2 592 627 A1

Description

FIELD OF THE INVENTION

[0001] The present invention is in the field of radiation physics. In particular, the present invention deals with the manipulation of γ-beams.

RELATED PRIOR ART

[0002] In nature, γ-radiation is produced by the decay of high energy states in atomic nuclei, also referred to as γ-decay. However, in the art the term "γ-radiation" is more generally used for any type of electromagnetic radiation having quantum energies beyond some lower boundary, irrespectively of the way the γ-radiation is generated. There is no generally accepted lower boundary of γ-radiation energies, but in the present disclosure, all electromagnetic radiation having a photon energy of 100 keV and beyond will be regarded as γ-radiation for simplicity. Below 200 keV, the electromagnetic radiation is often referred to as x-ray radiation, so there is a certain overlap between hard x-ray radiation and the lower part of the γ-spectrum.

[0003] γ-radiation has been employed in various fields of technology in the past. For example, γ-radiation is frequently used in radiation treatment of cancer. In radiation therapy apparatuses, usually electrons are accelerated in a linear accelerator to energies of several MeV and then directed onto a target, where x-ray and γ-radiation is generated in form of bremsstrahlung.

[0004] Also, γ-beams have been used in non-contact industrial sensors in various fields, including refining, mining, food industry and pulp and paper industries, in particular for measuring thicknesses, densities of materials or levels of fluids by assessing the absorption of γ-beams. Further, γ-beams are frequently used in medical imaging techniques, in particular positron emission tomography (PET) or single-photon emission computer tomography (SPECT). Currently, many new γ-beam sources are under development, so that it can be expected that γ-radiation will find increased use in many fields of technology in the near future. In particular, it turns out that very monochromatic γ-beams can be generated using Compton back-scattering of laser light from an electron beam. The γ-beams generated this way also have the advantage that the γ-photons are delivered into a rather small opening cone, see for example H.R. Weller et al., Prog. Part. Nucl. Phys. 62, 257 (2009).

[0005] While there are currently large advances in the generation of γ-beams, the possibilities to manipulate the γ-beam currently available are very limited. In the present state of the art, γ-beams can generally only be shaped by so-called collimators, which basically block parts of the beam with a very accurately shaped γ-absorbing material such as lead. However, simply blocking the part of the initial beam that does not fit the desired criteria implies that a large fraction of the initial γ-beam is discarded, making this way of collimation inherently inefficient. While it is further possible to manipulate a γ-beam by Bragg-reflection off a crystal, in this case the angle of deflection is limited by the Bragg-angle, but it is not possible to deflect a γ-beam by an arbitrary angle. Also, due to the divergence encountered in γ-beams, only a small portion of the initial beam that actually satisfies the Bragg-condition will be deflected, while the remainder of the beam (which is actually the most part of it) will simply pass through the crystal. So again, this manipulation of the γ-beam is inherently inefficient.

SUMMARY OF THE INVENTION

[0006] The problem underlying the invention is to provide a method and means for manipulating a beam of γ-photons. This problem is solved by using one or more refractive optical elements for one or more of shaping, deflecting, guiding by total internal reflection and monochromatizing a beam of γ-photons having an energy for which the energy dependent index of refraction of the material of said refracted optical element has a real part that is larger than 1. In preferred embodiments, the energy of the γ-photons is larger than 100 keV, preferably larger than 300 keV, more preferably larger than 500 keV, larger than 700 keV and larger than 1 MeV.

[0007] This problem is further solved by a focusing lens of claim 10, a focusing lens array of claim 11, a Fresnel lens or, a Fresnel zone plate of claim 13 and a monochromator of claim 14. Preferred embodiments are defined in the dependent claims.

[0008] While it is known to manipulate x-ray beams using refractive optical elements, it is so far generally accepted that at photon energies above say 200 keV, this is no longer possible. The reason is that according to the present understanding in the art, the index of refraction, which even in the x-ray regime is already very close to 1, rapidly converges even closer to 1 with increasing energy. The index of refraction n is usually written as $n = 1 + \delta + i\beta$, where δ is the deviation of the real part of n from unity. In the x-ray regime, the physical effect giving rise to δ is the virtual photo effect (Rayleigh scattering), which is therefore also referred to as "δ_{photo}" in the following. In the x-ray regime, δ_{photo} is negative, i.e. the index of refraction n is smaller than 1. A typical value of δ_{photo} at 80 keV and aluminum is -0.8×10^{-7} . This means

that refractive optical elements for use with x-rays are complementary to what one knows from ordinary glass optics for visible light, in the sense that e.g. a focusing lens for x-rays would have a concave shape instead of a convex shape as is familiar from "classical" optics, i.e. from the IR, visible or UV regime.

[0009] Further, it has been found that in the x-ray regime δ_{photo} converges inverse quadratically in the energy towards 0 according to the following formula:

$$\delta_{photo} = -2.70 * \frac{\lambda^2 * \rho * Z}{A} * 10^{-6} \qquad (1)$$

[0010] Herein, λ is the wavelength measured in angstrom, ρ is the density in g/cm^3, Z is the atomic number and A is the atomic mass in g. From the above equation (1) two facts are apparent. First, one immediately sees that even for x-rays, δ_{photo} will be rather small, i.e. the index of refraction n is already very close to unity. This is also why it had been believed for a long time that refractive optics for x-rays are not feasible. However, by designing x-ray lenses with a small radius of curvature R and by constructing arrays of a large number N of lenses, it turned out that lenses or lens systems with a reasonable focal length *f* could nevertheless be constructed. In particular, if R is the radius of a parabolically shaped concave lens used for focusing in the x-ray regime, the focal length can be defined as follows:

$$f = \frac{R}{2 * \delta * N} \qquad (2)$$

[0011] The second observation made from equation (1) is that with decreasing wavelength, i.e. increasing photon energy, δ_{photo} converges quadratically towards 0, as mentioned above. For this reason, it is currently believed that beyond approximately 200 keV, δ becomes prohibitively small such as to allow for any practically useful refractive optical elements.

[0012] However, the inventors have now found in very precise and quite involved experiments that surprisingly, for energies beyond some threshold, the value of δ increases again and in fact acquires a positive value. In other words, for photon energies above said threshold, the index of refraction is > 1 again, and the value of δ, i.e. the difference of n from unity, is large enough to allow for the design of useful refractive optical elements. Details of the experiments conducted by the inventors and the results thereof will be presented below. The exact value of the threshold where δ turns positive will depend on the material used. For Si, experiments presented below demonstrate that at about 700 keV, δ becomes positive and in fact acquires a value that is sufficiently large to allow for the design of useful refractive optical elements. For other materials, especially those with a higher atomic number Z, the threshold will be low. According to theoretical considerations, it is believed that for high-Z materials like Thorium, the threshold may be as low as about 100 keV only.

[0013] Further, the inventors have been able to attribute the unexpected positive δ beyond 700 keV (for Si) to a virtual pair creation, which has also been referred to as "Delbrück scattering" in the literature. This result is surprising as well, since in earlier works by J. S. Toll und J. A. Wheeler, it has been predicted that for energies of 1MeV the contribution of the virtual pair creation to the absolute value of δ was about a factor 10^3 smaller than the contribution due to the virtual photo effect (Rayleigh scattering) and should hence have a negligible effect on the index of refraction (see *J.S. Toll; The Dispersion Relation for Light and the Applications involving Electron Pairs, Princeton University (1952) unpublished).*

[0014] Up to now, this discouraging prediction has prevented experimentalists to search for a contribution of the virtual pair creation to the index of refraction. In view of the surprising results of the experiments conducted by the inventors, the original calculations of Toll and Wheeler and others have been revisited and it was found that some of the assumptions made in the calculations are not entirely correct, thus leading to a wrong prediction. This is also explained in more detail below.

[0015] The pivotal result of the findings of the inventors is hence that at energies beyond some threshold, of say a few hundred keV, the index of refraction will sufficiently deviate from unity such as to allow for refractive optical elements that can be used for shaping or deflecting a γ-beam. This is of tremendous practical importance, since refractive optics is very robust as compared to reflective optics, which always requires very precise alignment of the reflecting crystals. Further, since in this energy regime the index of refraction n is > 1, it is also possible to guide γ-beams by total internal

reflection. Note that this is not possible for x-rays, since in the x-ray regime, the index of refraction n is smaller than unity and hence x-ray beams can only be guided by total "external reflection".

[0016] When using the one or more refractive optical elements, the use employs the fact that the index of refraction n of the optical material has a real part > 1, or, in other words, that $\delta > 0$. This means that the design of the optical elements will be different from refractive x-ray optical elements and conceptually in fact more similar to ordinary light optics. For example, when using refractive optical elements for γ-photons having an energy of more than 700 keV, a focusing lens would have a convex shape, whereas an x-ray focusing lens has a concave shape.

[0017] Preferably, the shaping of the γ-beam comprises one or more of the following:

- focusing said γ-beam at least in one dimension,
- collimating said γ-beam at least in one dimension,
- diverging said γ-beam at least in one dimension, and
- separating a γ-beam into individual beamlets, in particular into parallel beamlets.

[0018] Note that in the present disclosure, a collimation is understood to shape a diverging beam to a less diverging, preferably parallel beam. Herein, the γ-beam may be focused or collimated using a convex lens or a plurality of convex lenses arranged in series, each convex lens having at least one, preferably two lens surfaces having a shape that is convex in at least one dimension. An example of a lens surface having a shape that is "convex in one dimension" would be a cylindrical lens which has a lens surface that is convex in a plane perpendicular to the cylinder axis but free of curvature in a plane parallel to the cylinder axis. Such lenses are also referred to as "1-D-lenses" and 1-D-lenses are sometimes advantageous from a manufacturing point of view, since they can for example be manufactured by vertically etching the lens surface from a wafer, as will be explained in more detail below. A lens with a lens surface that is convex in only one dimension would only focus the γ-beam in one dimension.

[0019] In a preferred embodiment, the convex lens has at least one, preferably two lens surfaces having a convex shape in two dimensions, and in particular, a rotation-ellipsoid shape. Such lens is referred to as a 2-D-lens, as it can focus the γ-beam in two dimensions. In a preferred embodiment, the convex lens is made from an embossed foil comprising one of Be, Al, Ni, Ta or Th as its main constituents. By embossing the foil, two-dimensional lenses can be manufactured easily and efficiently and with great precision of about 5 nm. Alternatively, such 2-D-γ-lens could also be made by micromachining.

[0020] Preferably, the tangential radius R at the apex of the lens is < 2000 μm, preferably < 1000 μm and more preferably between 5 μm and 500 μm. However, for contracted γ-beams, even smaller radii down to 1μm can be used.

[0021] Preferably, a number N of said convex lenses are arranged in series, for example stacked one behind the other in a lens holder. Herein, N is preferably between 2 and 10000, more preferably between 10 and 200. By stacking a large number of such convex lenses in series, a moderate focal length of the total stack of lenses can be achieved in spite of the rather small value of δ, thereby allowing for an efficient focusing or collimation of γ-beams. Since the absorption of γ-radiation is much less than that of x-ray radiation, the number of optical elements that can be arranged in series such as to accumulate the refractive effect of the individual refractive optical elements but still at a moderate total absorption is much higher for γ-radiation than for x-ray radiation.

[0022] Preferably, the body of said lens has a hole for ventilation, to thereby prevent the formation of air cushions and to avoid bending of the lens when mounting the lens array. The shape of the hole is not limited, as long as it allows for sufficient ventilation.

[0023] In a preferred embodiment, the γ-beam is focused or collimated by an array of lenses, wherein said array of lenses comprises at least one series arrangement of lenses allowing for being consecutively passed by a γ-beam, and wherein at least the majority of the lenses has at least one, preferably two lens surfaces having a convex shape in at least one dimension. For example, the "series arrangement" of lenses could be an arrangement of lenses along their optical axes. The term "lens surface" refers to the "entrance surface" and "exit surface" of the lens.

[0024] Herein, the mean radius of curvature of the convex shape or the tangential radius at the apex of the convex shape is preferably between 1 μm and 500 μm, preferably between 10 μm and 80 μm. Note in this regard that for manufacturing purposes, the convex lens surface may have a conical shape (in case of a 2-D-lens) or a triangular prism-like shape (in case of a 1-D-lens), in which case no tangential radius at the apex of the convex shape is defined, but a prism angle instead. In this case, we refer to the mean radius of curvature of the convex shape, which is defined as the radius of an arch or a sphere containing the apex and an edge portion of the lens surface.

[0025] Preferably, in the series arrangement, a number N of lenses are arranged in series such as to be consecutively passed by a γ-beam, wherein $N \geq 10$, preferably $N \geq 100$ and more preferably, $N \geq 300$. In some applications N may even be ≥ 1000. As before, by arranging a large number of lenses in series, the refractive power of the individual lenses adds up and the focal length of the total array is decreased.

[0026] Preferably, the array of lenses comprises a number M of series arrangements of lenses arranged in parallel, wherein $M \geq 2$, preferably $M \geq 4$ and more preferably $M \geq 10$. By providing a plurality of series arrangements of lenses

in parallel, it is possible to shape a γ-beam having a beam diameter that is considerably larger than the diameter of each individual lens. Note in this regard that due to the comparatively small radius of curvature of the lenses, the diameter of each individual lens will likewise be comparatively small. However, by arranging a plurality of series arrangements of lenses in parallel, an arbitrarily large beam cross section can be split up into a plurality of individual beamlets that are independently focused, collimated or shaped in another suitable way. The individually focused beamlets can then be further shaped, for example be deflected to be focused on a single spot or area, as is explained in more detail below.

[0027] In a preferred embodiment, the lens array is at least in part made from one or more wafers, in particular Si and/or Ge wafers, in which the lens surfaces are formed by etching. As is shown in detail in the experimental section below, both Si and Ge provide a sufficient index of refraction to construct useful refractive optical elements therefrom. While there are elements that would actually lead to a larger index of refraction, the advantage of using Si and/or Ge is that one can resort to well-established lithography and etching technology, in particular electron beam lithography, to efficiently and precisely manufacture miniature structures, thereby allowing to manufacture arrays of very large numbers of lenses with a very small radius of curvature in a cost efficient way. Also, due to this manufacturing, the individual lenses can be aligned very precisely.

[0028] Preferably, the one or more wafers has/have a thickness between 20 μm and 200 μm, preferably between 50 μm and 100 μm. If the thickness is below 100 μm, it is possible to etch precise vertical walls constituting the lens surfaces, for example by ion beam deep etching or the like. Note that alternative manufacturing methods, including improved methods that will become available in the future are also possible.

[0029] In a preferred embodiment, the lens array is at least in part made from a stack of a plurality of identically etched wafers, wherein the wafers of the stack are preferably grown or fused together. This allows obtaining a total thickness of the stack of wafers of for example 5 mm or more, preferably 8 mm or more, thereby allowing to shape a γ-beam having a corresponding beam width. If desired, even larger stacks of identically etched wafers can be formed.

[0030] Owing to the vertical etching technique, the lens surfaces have a convex shape only in one dimension, i.e. are 1-D lenses only. This means that the lens array can only focus a γ-beam in the plane of the wafer but not in a plane perpendicular to the wafer plane. However, in a preferred embodiment, the γ-beam is focused or collimated by two arrays of lenses according to one of the embodiments described above, which are arranged in series and are oriented with respect to each other such that each of the two lens arrays focuses or collimates a γ-beam within different planes, such as two perpendicular planes.

[0031] In a preferred embodiment, the γ-beam is deflected by an array of prisms, wherein the array of prisms comprises at least one series arrangement of prisms allowing for being consecutively passed by a γ-beam. By arranging a plurality of prisms in series, the minute deflections occasioned by each individual prism add up to provide for a considerable total deflection by the array of prisms as a whole.

[0032] Preferably, a number N of prisms are arranged in series, such as to be consecutively passed by a γ-beam. Herein, N may be ≥ 2, preferably ≥ 10 and more preferably ≥ 100. The suitable number of N also depends on the angle of the prism. However, if desired, the number of prisms arranged in series can be easily increased to hundreds or even thousands, in view of the comparatively small absorption of γ-radiation in matter.

[0033] Preferably, at least the majority of prisms in the array of prisms has a wedge-shape with a base surface having a triangular shape. Herein, the height of the triangular shape is preferably smaller than 200 μm, preferably smaller than 50 μm. The base surface may further have an isosceles triangle shape, wherein the angle γ between the two equal sides of said isosceles triangle is preferably between 5° and 120°, more preferably between 15° and 90°.

[0034] Similar to the lens array, the array of prisms may also comprise a number M of series arrangements of prisms arranged in parallel, wherein $M \geq 2$, preferably $M \geq 4$ and more preferably $M \geq 10$. Again, this allows deflecting a large diameter beam with a suitably large number of series arrangements of comparatively small prisms arranged in parallel.

[0035] Similar to the lens arrays described above, the array of prisms is likewise preferably at least in part made from one or more wafers, in particular Si and/or Ge wafers, in which the prisms are formed by etching. Herein, the one or more wafers has/have a thickness between 20 μm and 200 μm, preferably between 50 μm and 100 μm, and the array of prisms may at least in part be made from a stack of a plurality of identically etched wafers wherein said wafers of said stack are preferably grown or fused together such as to yield a total thickness of the stack of 5 mm or more, preferably 8 mm or more.

[0036] In a preferred embodiment, a lens array and a prism array, each according to one of the embodiments described above, can be combined in a refractive optical element. In particular, the refractive optical element may comprise a lens array as described above that is configured for separating a γ-beam into individual beamlets and focusing the individual beamlets by means of a plurality of series arrangements of lenses arranged in parallel. The refractive optical element may further comprise a prism array as described above, that is arranged such as to receive and deflect the individual beamlets. In particular, the individual beamlets may be deflected by the array of prisms such as to converge the individual beamlets at a common focal point or focal area.

[0037] In a preferred embodiment, the γ-beam is shaped using a one-dimensional or two-dimensional Fresnel lens. In particular, a two-dimensional Fresnel lens can be used for focusing or collimating a γ-beam. In this case, the Fresnel

lens has a convex shape in its central zone, wherein the radius of curvature in the central zone is preferably between 1 μm and 200 μm. Herein, the "radius of curvature" may refer to the mean radius of curvature in the central zone or the radius of curvature at the apex of the central zone. The advantage of a Fresnel lens is that it allows reducing lens material and hence limits the absorption of γ-energy by the lens. Preferably, after each phase advance by 2 π, a jump back in thickness occurs.

[0038] In a preferred embodiment, a γ-beam is shaped using a Fresnel zone plate having zones of at least two different materials with different values of atomic number Z and atomic mass A, thus leading to a different phase advance. Herein, the γ-beam may be focused or collimated using a Fresnel zone plate, wherein the central zone is a zone of larger optical phase advance δ.

[0039] In a preferred embodiment, the γ-beam is provided by a Compton back-scattering of laser light from an electron beam. Generating a γ-beam by Compton back-scattering leads to γ-beams having comparatively small opening angles and energy spread. In addition, the apparative effort necessary for this type of γ-beam generation is still moderate. Accordingly, the refractive optical elements as described herein can be ideally employed in combination with a γ-source generating a γ-beam by Compton back scattering of laser light from an electron beam. In fact, with the new γ-optics, seeded quantum FEL γ-beams with much improved brilliance become possible.

[0040] The novel refractive optical elements for use with γ-photons can further be employed in combination with diffractive optical means. A very important example of such a combination is a novel monochromator for monochromatizing a beam of γ-photons. While the monochromator is discussed with reference to γ-photons in the following, it is emphasized that the same design can also be used for x-ray photons or low energy neutrons In particular, the monochromator disclosed herein can be used for photons having energies as low as 10 keV and neutrons having energies below 1 eV.

[0041] The monochromator comprises a plurality of pairs of Laue-crystals, each pair of Laue-crystals having

- a first Laue-crystal for diffracting a portion of an incoming γ-beam that meets the Bragg-condition and transmitting the remainder of the incoming γ-beam without diffraction, and
- a second Laue-crystal arranged with respect to the first Laue-crystal such as to allow for a further Laue-diffraction of the beam portion that was Laue-diffracted at the first Laue-crystal of said pair of Laue-crystals.

[0042] Herein, the first Laue-crystals of all pairs of Laue-crystals are parallel to each other and the second Laue-crystals of all pairs of Laue-crystals are parallel to each other as well. The first Laue-crystals of the pairs of Laue-crystals are arranged in series with refractive deflection means arranged inbetween such that the part of the beam that is transmitted without diffraction by one of said first Laue-crystals is deflected prior to impinging on the next first Laue-crystal in said series of first Laue-crystals.

[0043] Note that the "Laue-diffraction" is equivalent to "Bragg-reflection", except that the diffracted beam passes through the crystal. A Laue-diffraction can be regarded as a Bragg-reflection at crystal planes that are vertical to the crystal surface. The Bragg-condition is known as $m \cdot \lambda = 2d \cdot \sin\theta$, where m is a positive or negative integer, d is the lattice spacing, θ is the angle between the impinging beam and the lattice plane, and λ is the wavelength of the photon.

[0044] Monochromatizing a γ-beam with two Laue-crystals is inherently done in so-called two-crystal spectrometers, also referred to as double crystal or Laue spectrometers, as described in *E.G. Kessler et al., Nucl Inst. Meth. A 457, 187 (2001),* where, however, only a single pair of Laue-crystals is used. If the two Laue-crystals are parallel to each other, this is referred to as the "non-dispersive geometry". The portion of the γ-beam that satisfies the Bragg-condition with regard to angle and wavelength (i.e. energy) is Laue-diffracted at the first Laue-crystal. The remainder of the beam that does not satisfy the Bragg-condition will simply be transmitted without diffraction by the first Laue-crystal. Note that the Laue-condition and Bragg-condition are equivalent and are hence used interchangeably herein. In the non-dispersive geometry, i.e. when the first and second Laue-crystals of the pair are parallel to each other, the planes of the two crystals are parallel, too, so that all wavelengths and angles that are diffracted by the first crystal simultaneously satisfy the Bragg-condition at the second crystal and are diffracted likewise.

[0045] When the second Laue-crystal is, however, inclined with regard to the first Laue-crystal by e.g. twice the Bragg-angle of the desired wavelength (energy), only the photons with the corresponding wavelength will obey the Bragg-condition at the second crystal as well and hence be diffracted, while photons with other wavelengths will be transmitted without diffraction by the second Laue-crystal. This configuration of the Laue spectrometer is called the "dispersive mode" for obvious reasons and inherently acts as a monochromator with a very narrow rocking curve and very small band width of typically 10^{-6}.

[0046] However, the efficiency of such a monochromator is very limited, since the first Laue-crystal is very selective with regard to impinging angles in the sense that only photons within a very limited angular range will actually be diffracted by the first Laue-crystal. What is more, the angular range that is "accepted" by the first Laue-crystal decreases with energy. For γ-energies above 700 keV that are of particular interest in the framework of the present invention, this means that only γ-beams deviating from the Bragg-angle by several 10 nrad will actually be "accepted", i.e. diffracted by the

first Laue-crystal. Since the best collimated γ-beams typically have divergences in the range of some tens of μrad, this means that the ordinary Laue spectrometer will miss the biggest part of the γ-radiation, irrespectively of the photon energy, due to the angular spread.

[0047] In the monochromator according to an embodiment of the invention, a plurality of pairs of Laue-crystals is employed, each pair having a first and a second Laue-crystal. Further, the first Laue-crystals of all pairs of Laue-crystals are arranged in series with refractive deflection means arranged inbetween such that the part of the beam that is transmitted without diffraction by one of the first Laue-crystals - because it may be outside the angular acceptance range of said first Laue-crystal - is deflected prior to impinging on the next first Laue-crystal in said series. This deflection will lead to a shift of the undiffracted transmitted beam in angular space before impinging on the next first Laue-crystal. Since all first Laue-crystals are parallel to each other, a portion of the γ-beam that was transmitted without diffraction by the previous first Laue-crystal will now fall into the angle acceptance range and will be Laue-diffracted by the next first Laue-crystal in the series and - after further Laue-diffraction at the corresponding second Laue-crystal of the pair - contribute to the monochromatized γ-beam. Accordingly, for the same incident γ-beam, the efficiency of the monochromator is (except for absorption losses) increased over that of an ordinary Laue spectrometer by a factor corresponding to the number of Laue-crystal pairs.

[0048] Preferably, the refractive deflection means arranged between consecutive first Laue-crystals in said series of first Laue-crystals are adapted to deflect the beam by an angle α that is larger than but still reasonably close the angular acceptance width of the first Laue-crystal for the desired γ-photon energy. In particular, the angle α is given by 5 nrad $< \alpha <$ 200 nrad, preferably 10 nrad $< \alpha <$ 100 nrad

[0049] In a preferred embodiment, the number of pairs of Laue-crystals employed in the monochromator is at least 5, preferably at least 10 and more preferably at least 50. As mentioned before, the higher the number of pairs of Laue-crystals, the larger is the efficiency of the monochromator. In practice, one will have to find a suitable compromise between optimum efficiency and structural effort.

[0050] Preferably, the first and second Laue-crystals of each pair of Laue-crystals are either parallel to each other, which corresponds to the non-dispersive mode, or inclined with respect to each other such as to allow for an energy selection by two consecutive Laue diffractions, and in particular inclined by twice the Bragg-angle of the desired wavelength. This corresponds to the dispersive geometry. In practice, the dispersive geometry is preferably used for monochromatization, while the non-dispersive mode may be used to align all optical elements, in particular the deflection means. In a particularly preferred embodiment, the first and second Laue-crystals are shiftable between the two configurations. This will for example allow precisely adjusting the refractive deflection elements in the parallel mode and then decreasing the energy width by shifting the first and second Laue-crystals with respect to each other to the dispersive geometry.

[0051] In a preferred embodiment, all first Laue-crystals are part of one fixed first unit, and all second Laue-crystals are part of one fixed second unit. Herein, the first and second units are preferably each made from a single crystal block, as this ensures that all first crystals and all second crystals are mutually parallel with each other.

[0052] In a preferred embodiment, both blocks are taken from the same ingot, which allows for a perfect match of the first and second Laue-crystals. The Laue-crystals may in particular consist of Si and/or Ge. Also, preferably a collimating lens, lens stack or lens array is arranged upstream of the monochromator such as to parallelize or at least reduce the divergence of the beam prior to entering the monochromator. This way, the efficiency of the monochromator can be dramatically increased. Herein, one of the collimating lenses, lens stacks or lens arrays described above may be employed.

[0053] From a conceptional point of view, it is easiest to think of the monochromator as a series of completely separate Laue-spectrometers, where each γ-beam transmitted without diffraction by the first Laue-crystal of a given Laue-spectrometer is deflected and then inputted into the first Laue-crystal of the following Laue-spectrometer. However, since the angle between γ-beams transmitted undiffracted by and Laue-diffracted by a Laue-crystal will be very small, a spatial separation of the pairs of Laue-crystals will in practice be difficult to achieve. Instead, in practice the geometry will rather be such that a beam that has already been Laue-diffracted by a first (second) Laue-crystal of one pair passes a first (second) Laue-crystal of another pair of Laue-crystals for the practical reasons that it is difficult to keep these Laue-crystals of the further pair out of the way of the diffracted beam. However, since all first (second) Laue-crystals are parallel to each other, this would imply that the already Laue-diffracted beam is Laue-diffracted at the fist (second) Laue-crystal of this other pair of Laue-crystals again. According to an embodiment of the invention, this is prevented by ensuring that a beam that has already been Laue-diffracted by a first (second) Laue-crystal of one pair is deflected using a refractive optical element prior to passing a first (second) Laue-crystal of another pair of Laue-crystals. This way, it can be ensured that the beam is diffracted only once at a first Laue-crystal and once at a second Laue-crystal forming the abovementioned pair of Laue-crystals.

[0054] In one embodiment, the refractive optical elements arranged between two adjacent first Laue-crystals for deflecting a beam transmitted without diffraction by the previous first Laue-crystal in said series are arranged to also deflect the beam that is Laue-diffracted by said previous first Laue-crystal. Accordingly, this way it can be ensured that the

Laue-diffracted beam is not Laue-diffracted at any further first Laue-crystal in said series, because after deflection, i.e. an angle change, it no longer obeys the Bragg-condition.

[0055] In a preferred embodiment, the first and second Laue-crystals are arranged in the monochromator such that the first and second Laue-crystals of each pair are adjacent to each other.

[0056] In an alternative embodiment, the first and second Laue-crystals are arranged in the monochromator such that all first Laue-crystals are arranged in a series and all second Laue-crystals are arranged in a further series that is arranged downstream of the series of first Laue-crystals with regard to the propagation direction of the beam. Further, first refractive deflection means are placed between each two neighbouring first Laue-crystals, and second refractive deflection means are placed between each two neighbouring second Laue-crystals. Herein, the second refractive deflection means in the n^{th} gap between neighbouring second Laue-crystals when counted in opposite propagation direction of the beam is adapted to compensate for the deflection provided by the first refractive deflection means in the n^{th} gap between neighbouring first Laue-crystals when counted in propagation direction of the beam. With this geometry, each beam that is Laue-diffracted at any first Laue-crystal may pass through all downstream first and second Laue-crystals while it is still ensured that it is only Laue-diffracted by the corresponding second Laue-crystal of the pair. As will be explained in more detail below with reference to a preferred embodiment, in this geometry, the most upstream one of the first Laue-crystals and the most downstream one of the second Laue-crystals form a pair, the second most upstream one of the first Laue-crystals and the second most downstream one of the second Laue-crystals form a further pair and so on.

SHORT DESCRIPTION OF THE FIGURES

[0057]

Fig. 1	is a schematic perspective view showing a Laue-spectrometer used for measuring the index of refraction.
Fig. 2	is a plan view onto the Laue-spectrometer of Fig. 1 with and without a deflecting prism arranged between the crystals.
Fig. 3	shows intensity-angle curves of a beam that is outputted from the Lauespectrometer of Fig. 1 with and without a deflecting prism in the light path.
Fig. 4	is a table summarizing the values of δ for Si measured at nine different energies.
Fig. 5	is a diagram summarizing the energy dependents of various cross sections contributing to the index of refraction.
Fig. 6	is a diagram showing the expected value of $\|\delta\|$ as a function of energy as caused by the coherent virtual photo effect, coherent virtual Compton effect, coherent virtual pair effect and corrected pair creation.
Fig. 7	is a diagram showing the measured values of $\|\delta\|$ for different energies.
Fig. 8(a) and (b)	show a cross sectional view and a perspective view of a 2-D lens according to an embodiment of the invention.
Fig. 9(a) and (b)	show a plan view and a perspective view of a lens array according to an embodiment of the invention.
Fig. 10 (a) and (b)	show a plan view and a perspective view of a wedge array according to an embodiment of the present invention.
Fig. 11	shows a combination of a lens array and two wedge arrays according to the embodiment of the invention.
Fig. 12 (a) and (b)	show a plan view and a perspective view of a 1-D Fresnel lens according to an embodiment of the invention.
Fig. 12 (c)	shows a perspective view of a 2-D Fresnel lens according to an embodiment of the invention.

Fig. 13 shows a sectional view of a Fresnel zone plate according to an embodiment of the invention.

Fig. 14 shows a schematic view of a double crystal spectrometer in the non-dispersive and dispersive modes.

Fig. 15 shows examples of rocking curves at energies of 100 keV, 500keV and 1000 keV for a 2.5 mm Si crystal.

Fig. 16 is a schematic representation of a monochromator according to one embodiment of the invention.

Fig. 17 is a series of diagrams showing intensity-angle profiles of a beam in various places within the monochromator of Fig. 16.

Fig. 18 is a schematic angle-energy diagram illustrating the operation of a monochromator according to an embodiment of the invention.

Fig. 19 is a schematic sectional view of a monochromator according to a further embodiment of the invention.

Fig. 20 is a schematic sectional view of a further embodiment of the monochromator of the invention.

Fig. 21 is a schematic perspective view showing one of the crystal units of the monochromator of Fig. 20

DESCRIPTION OF THE PREFERRED EMBODIMENTS

[0058] For the purposes of promoting an understanding of the principles of the invention, reference will now be made to the preferred embodiments illustrated in the drawings and specific language will be used to describe the same. It will nevertheless be understood that no limitation of the scope of the invention is thereby intended, such alterations and further modifications in the illustrated devices and methods and such further applications of the principles of the invention as illustrated therein being contemplated as would normally occur now or in the future to one skilled in the art to which the invention relates.

[0059] The present invention is based on the surprising finding that for γ-energies larger than some material dependent threshold, the real part of the index of refraction is larger than unity and in fact differs from unity by a sufficient extent, such as to allow for the construction of refractive optical elements. In Si, this threshold is at approximately 700 keV

[0060] In section I below, experiments conducted by the inventors giving empirical support for the technical effect underlying the invention will by summarized and quantitative results will be presented.

[0061] In section II, a theoretical explanation of the physics underlying this technical effect will briefly be presented and compared with earlier theoretical work that led to conclude that the technical effect underlying the invention would not exist.

[0062] In section III, finally, preferred embodiments of refractive optical elements of the invention and preferred uses thereof will be described in detail.

I. Measurement of index of refraction in experiment

[0063] The inventors have performed index of refraction measurements at the GAMS double crystal spectrometer at the high-flux reactor of the Institute Laue - Langevin (ILL) in Grenoble. The spectrometer is installed at the exit "H7" of the tangential beam tube "H6/H7". Samples for the creation of γ-radiation have been placed in a thermal neutron flux of $4x10^5$ $s^{-1}cm^{-2}$. Typically, three samples with a total mass of 10 g and a surface of about 30 cm^2 were used. When exposed to the neutron flux, the samples undergo a thermal neutron capture reaction and consequently emit monochromatic γ-beams, wherein the energy of the γ-photons depends on the chemical and isotopic composition of the sample. The emission rates of a particular γ-energy can be as high as 10^{15} s^{-1}.

[0064] In the experiment, very intense transitions of ^{36}Cl and $^{156,\ 158}$Gd were used, resulting in strong γ-beams with energies of 517 keV, 786 keV, 1165 keV 1951 keV for ^{36}Cl and 80 keV, 182 keV, 606 keV, 780 keV, 896 keV and 944 keV for $^{156,\ 158}$Gd.

[0065] The γ-beam emerging from the sample was collimated over a total distance of 17 m with a cross section of $4x20$ mm^2 and then fed into the GAMS double crystal spectrometer 10 that is schematically shown in Fig. 1. In Fig. 2, a schematic top view of the double crystal spectrometer 10 with and without a prism 18 placed in the beam path are shown. The GAMS spectrometer was developed over many years as an ultra high resolution γ-spectrometer for measuring

of, for example, absolute wavelength standards or neutron binding energies, see E.G. Kessler et al., Nucl Inst. Meth. A 45 7, 187 (2001).

[0066] The double crystal spectrometer 10 comprises two perfect single crystals 12, 14. The lattice spacing d of the crystals 12, 14 is known to be homogeneous with $\Delta d/d < 10^{-7}$. The γ-beam impinging on the first crystal 12 is shown at reference sign 16. The γ-beam 16 consists of two parts that are symbolically represented by individual rays 16a, 16b, of which one part 16b passes a prism 18 arranged between the crystal slabs 12 and 14, while the other part 16a bypasses the prism 18.

[0067] Upon impinging on the first crystal 12, a part of the γ-beam 16 that obeys the Bragg-condition is Laue-diffracted at the first crystal 12. In Fig. 1 only the Laue-diffracted γ-beam is shown. Note, however, that the biggest part of the γ-beam will actually not obey the Bragg-condition and hence simply pass through the first crystal 12 and not play any further role in the experiment.

[0068] Accordingly, the first crystal 12 is used to select a proper energy and to obtain a γ-beam with an extremely low divergence of approximately 10 nrad .

[0069] The second crystal 14 is rotated stepwisely through a small angular range around the Bragg-angle, which is also referred to a "rocking" of the second crystal. The intensity profile of the γ-beam that is Laue-diffracted at the second crystal 14 is recorded as a function of crystal angle using a Ge detector. The corresponding measured intensity versus rocking angle profile for one γ-photon energy is shown in Fig. 3, where the upper curve represents the intensity profile of beam 16a that bypassed the prism 18 and the lower curve corresponds to the intensity profile of the beam part 16b that was deflected by the prism 18.

[0070] The intensity profiles of Fig. 3, also referred to as "rocking curves" in the art, show typical oscillations of the dynamical diffraction profiles which are the so-called "Pendellösung" oscillations. For more details, reference is again made to *E.G. Kessler et al., Nucl Inst. Meth. A 457, 187 (2001).*

[0071] In Fig. 3, the angle is measured by a number of optical fringes in a way further explained in the article by E.G. Kessler et al. cited above. However, what is clearly seen from Fig. 3 is that the two rocking curves for the beam portions 16a and 16b are shifted with respect to each other in angular space, which is due to a deflection of beam portion 16b in the prism 18. From this deflection, the index of refraction of the material of the prism 18 can be determined for the respective γ-energy. Note that in the experiments, the switching between the beam parts 16a and 16b was effected with a lead shutter that was installed on the collimation system behind the spectrometer 10. This ensures that the movement of the lead shutter is mechanically decoupled from the spectrometer 10.

[0072] The measurement has been repeated for ten different energies and for an Si-prism. The results of the measurements are summarized in the table in Fig. 4. Also, the measured values of δ vs. energy for the Si-prism 18 are shown in Fig. 7 to be discussed in more detail below.

II. Theoretical prediction of index of refraction by dispersion relations

[0073] In this section, we use dispersion relations to calculate the real part δ of the deviation of the refraction index from 1. For this, we introduce the outgoing complex forward scattering amplitude $A_f(E_\gamma) = A_{rf}(E\gamma)+iA_{if}(E_\gamma)$, with the real part $A_{rf}(E_\gamma)$ and the imaginary part $A_{if}(E_\gamma)$. The virtual processes with coherent cross sections σ_{sca} contribute to the real part A_{rf}, while the real processes with cross sections σ_{abs} as well as the inelastic virtual processes contribute to the imaginary part A_{if} of the coherent scattering amplitude. The Kramers-Kronig dispersion relations yield:

$$A_{rf}(E_\gamma) = \frac{E_\gamma^2}{\pi(4\pi^2\hbar c)^2} \lim_{\epsilon\to 0+} \int_0^\infty \frac{A_{if}(E)dE}{E(E^2-(E_\gamma+i\epsilon)^2)} \quad (3)$$

[0074] By the optical theorem, the imaginary part of the forward-scattering amplitude is related to the total absorption cross section: $\sigma_{abs}(E_\gamma) = 2\cdot\lambda\cdot A_{if}(E_\gamma)$, or in other words, $A_{if}(E) = \left(\frac{E}{4\pi\hbar c}\right)\cdot\sigma_{abs}(E)$. We thus obtain

$$A_{rf}(E_\gamma) = \frac{E_\gamma^2}{2\pi^2\hbar c} \lim_{\epsilon \to 0+} \int_0^\infty \frac{\sigma_{abs}(E)dE}{E^2 - (E_\gamma + i\epsilon)^2} \quad (4)$$

[0075] Equation (4) thus connects the total absorption cross section $\sigma_{abs}(E)$ with the forward coherent scattering cross section

$$\frac{d\sigma_{sca}}{d\Omega}(forward) = |A_{rf}(E_\gamma)|^2 \quad , (5)$$

which is in turn related to the real part of the index of refraction $\delta(E_\gamma)$ as follows:

$$\delta(E_\gamma) = \frac{\lambda^2}{2\pi} \cdot N_c \cdot A_{rf}(E_\gamma) \quad , (6)$$

where N_C is the number of scattering centers per volume.

[0076] The absorptive part $\beta(E_\gamma)$ of the index of refraction $n(E_\gamma)$ is given by $\beta(E_\gamma) = (\mu\lambda\gamma)/(4\pi)$, where $\mu = N_C \cdot Z \cdot \sigma_{abs}$ is the linear absorption coefficient. With these formulas one can now calculate the corresponding real parts σ_{photo}, $\delta_{Compton}$ and δ_{pair} of the index of refraction (or more precisely, its deviation from unity) for the three processes photo effect, Compton effect and pair creation.

[0077] For calculating explicit values, the corresponding scattering cross sections are needed. Fig. 5 shows the energy dependent cross sections for the photo effect, Rayleigh scattering, Compton scattering and pair creation as known from experiment and available in the literature. Further, in the dotted curve, Fig. 5 shows a "corrected pair creation" cross section that has been recently measured close to the threshold by one of the inventors (M. Jentschel et al., accepted for publication in Phys. Ref. C Rapid Communications). Finally, Fig. 5 also shows the estimated cross sections due to the elastic and inelastic virtual pair creation, which is referred to as "Delbrück scattering" in the following.

[0078] In this theoretical analysis, the important Delbrück scattering is divided into an elastic part, where in a Mössbauer-like recoilless scattering the recoil is taken up by the total crystal $\sigma_{Delb,elas}$ and an inelastic cross section $\sigma_{Delb,inelas}$, where the scattered quantum has lost the recoil energy to the nucleus. For a large fraction of recoilless emission, the recoil energy E_R has to be smaller than $k\Theta_D$, where Θ_D is the Debye temperature, see R.L. Mössbauer, Recoilless Nuclear Resonance Absorption, Ann. Rev. Nucl. Sci. 12, 123 (1962*) and* R.L. Mössbauer, Z.f. Physik, 151, 124 (1958*)*.

$$E_R = \frac{E_\gamma^2 sin(\Theta_{elas})^2}{2Mc^2} < k\Theta_D \approx 20meV$$

[0079] Thus $\Theta_{elas} \approx 10^{-2}$ for 1 MeV and decreases with $1/E_\gamma$. The forward-peaked Delbrück scattering cross section drops off fast for $\Theta_{max} > 0.2$ $(0.5MeV/E_\gamma)$ (see H.A. Bethe and F. Rohrlich, Phys. Rev. 86, 10 (1952*)*, again scaling with $1/E_\gamma$. Also, the scaling with the γ-energy for low and high E_γ is known (see F. Rohrlich et al., Phys. Rev. 86, 1 (1952*)*. One can calculate the integrated cross sections up to Θ_{elas} for the elastic Delbrück scattering $\sigma_{Deln,elas}$ and beyond Θ_{elas} for the inelastic Delbrück scattering $\sigma_{Delb,inelas}$. Both are shown in Fig. 5.

[0080] In Fig. 6, the absolute value of $|\delta|$ according to the virtual photo effect, virtual Compton effect, virtual pair effect and corrected pair creation are shown. Herein, δ_{photo}, i.e. the contribution due to the coherent virtual photo effect, has been taken from experimental measurements, i.e. equation (1).

[0081] The strongly rising pair creation cross section and inelastic Delbrück scattering results in a positive δ_{pair}, while

the decreasing cross sections of the photo effect and Compton scattering result in a negative δ_{photo} and a negative $\delta_{Compton}$. The surprising result is that $|\delta_{pair}|$ becomes larger than $|\delta_{photo}|$. Historically, in 1952, J.S. Toll and J.A. Wheeler predicted wrongly for lead (Z=82) and 1 MeV quanta that $|\delta_{pair}|$ should be about a factor of 10^3 smaller than $|\delta_{photo}|$, preventing experimentalists from searching for a δ_{pair} contribution. Via dispersion relations they calculated with the Thomas-Reiche-Kuhn sum rule that the real scattering amplitude due to the photo effect $A_{rf}\ photo = Z \cdot r_0$. This would result in a Z^2 dependence of δ_{photo}, while experimentally only a linear dependence in Z is observed (see Eq. (1)). In particular, they assumed a coherent interaction of the γ quantum with all Z electrons, however, if the area of λ_γ^2 is a factor of about 100 smaller than the area of the atom, in fact a very local and not a coherent interaction occurs. Furthermore, one obtains $A_{rf,\ photo} = 0.7 \cdot r_0$ from the experimental measurements of δ_{photo} from Eq. (1). One can understand this factor of 0.7 because the total energy-integrated electron absorption cross section divides up into a stronger cross section of the photo effect, but also a cross section for the Compton effect. Thus for Z=82, the predicted δ_{photo} is reduced by a factor of $82/0.7 \approx 120$.

[0082] On the other hand, δ_{pair} was predicted about a factor of 10 too small by neglecting in the absorption cross section, besides the cross section for pair creation, the cross section for inelastic Delbrück scattering. When calculating the real scattering amplitude via dispersion relations, this leads to much smaller values. The same omission occurred in the papers by Bethe et al. H.A. Bethe and F. Rohrlich, Phys. Rev. 86, 10 (1952) and by Rohrlich et al. F. Rohrlich et al., Phys. Rev. 86, 1 (1952).

[0083] A further increase of δ_{pair} and $A_{rf,\ pair}(E_\gamma)$ occurs, because experimentally a strong enhancement of pair creation close to threshold over the predicted Bethe-Heitler cross section is observed in recent measurements by one of the inventors referred to above. Since the contribution to δ in Eq. (5) becomes very large if E_γ is close to E, and if σ_{abs} is steeply sloped as a function of E, this strong increase of the absorption cross section close to $2 \cdot mc^2$ increases the value of δ_{pair} significantly. Thus the measured similar absolute values of δ_{pair} and δ_{photo} can be explained naturally, using the dispersion relations. As shown in Fig. 6 δ_{pair} has a rather constant energy dependence at low energies, which then rises to maximum values between 1 MeV and 2 MeV, followed by a fall off with E_γ^{-1} for higher γ-energies. We expect a scaling of δ_{pair} due to the Bether-Heitler pair creation with Z^2 (see H.A. Bethe et al., Proc. Roy. Soc. (London), 146, 83 (1934)). A further factor 1/A is introduced when determining the number of nuclei per reference volume via the density p. Thus we can parameterize $\delta_{pair} = c_{pair} \cdot \frac{Z^2}{A} \cdot \rho$ with a universal constant c_{pair} and p measured in g/cm^3. In our measurement we obtained $C_{pair} = (5 \pm 0.5) \cdot 10^{-7}$ for 1 MeV. Since $|\delta_{pair}/\delta_{photo}|$ increases proportional to Z, we expect the switchover to positive δ for high Z materials at smaller energies.

[0084] Accordingly, while the switchover of δ to positive values has been found to be at about 700 keV for Si, it is believed that positive δ can be obtained at considerably lower energies for high Z materials.

III. Description of new optical elements

[0085] The experimental results as presented in section I. above and the theoretical explanation thereof in the preceding section II. led the inventors to propose refractive optical elements for manipulating a beam of γ-photons having an energy beyond the threshold where δ becomes positive. Suitable optical elements will be described in more detail in the present section III.

[0086] Note in this regard that the surprising and non-obvious behaviour of the index of refraction discovered by the inventors calls for new designs of optical elements that are currently not used. In particular, while for example focusing lenses for x-rays have been developed in the past, they cannot be employed for focusing γ-photons beyond say 700 keV, because the qualitative behaviour of the index of refraction changes as compared to the x-ray regime. Namely, as was shown before, the dominant contribution to the index of refraction in the x-ray regime δ_{photo} has a negative sign, meaning that the real part of the index of refraction is smaller than one. For γ-photons beyond the aforementioned threshold, however, the dominant physical effect contributing to the index of refraction is pair creation yielding a δ_{pair} that is positive, and to a total index of refraction having a real part that is larger than one. Accordingly, for γ-beams above said threshold, we can expect a phase advance rather than a phase retardation for the scattered wave, similar to what is known from ordinary light optics.

[0087] Needless to say, prior art optical elements that have been used for light optics will not be suitable for manipulating γ-beams either, since the curvatures of e.g. glass optical focusing lenses for use in the IR, visible or UV regime would be much too small in order to obtain any noticeable effect for γ-rays.

[0088] Instead, new optical elements for the specific γ-radiation beyond the threshold energy need to be devised, and the currently most preferable ones are briefly described below. It is nevertheless understood that the scope of the invention is not limited to the specific optical elements described below. Instead, based on the behaviour of the index of refraction as shown in Fig. 7, it is possible to devise many more optical elements for use with γ-photons as desired. In fact, a plethora of diffractive x-ray optics applications has been proposed, see e.g. D.M Paganin, Coherent X-Ray Optics, Oxford University Press, Oxford, (2006*),* and with the knowledge of the new diffractive index valid beyond the positive-δ-threshold such as 700 keV in case of Si, for example, they can be "translated" to the γ-regime.

III.1 2-D focusing lens

[0089] In Fig. 8, a cross section (Fig. 8(a)) and a perspective view (Fig. 8(b)) of a 2-D focusing γ-lens according to an embodiment of the invention is shown. The γ-lens is "two-dimensional" in the sense that it is optically active in two dimensions, meaning that the lens surfaces are curved in two orthogonal sections A-A (shown in Fig. 8(a) and B-B (not shown). This means that a γ-beam will be focused in two dimensions, such as to converge to a focal "point". This is to distinguish the lens from 1-D-lenses described below, where the beam is only shaped in one dimension but left unaffected in another dimension such as to, for example focus a circular beam onto a line rather than onto a point.

[0090] The lens 22 is made from a nickel foil that is squeezed between two profiled pistons to acquire the convex shape that is particularly apparent from Fig. 8(a). With this embossing technique, the lens 22 can be manufactured comparatively easily and cheaply and to a high precision of about 100 nm. The lens surfaces 24 and 26 of the lens 22 have a rotational ellipsoid shape that is characterized by an inscribed tangential radius at its apex 30. Preferably, the radius R at the apex 30 is smaller than 2000 μm, preferably smaller than 1000 μm and preferably between 5 μm and 500 μm. The smaller the radius of curvature (i.e. the larger the curvature), the smaller the focal length.

[0091] As is further seen in Fig. 8, the lens 22 has mounts 32 at two sides, which may have a length of about 10 mm. With these mounts, a plurality of lenses 22 can be stacked one behind the other in a lens holder (not shown), to thereby add up the focusing power of multiple lenses. In practice, several hundreds or even a thousand of lenses 22 can be manufactured and stacked one behind the other.

[0092] As is further seen in Fig. 8(b), a hole 34 for ventilation is provided in the body of the lenses 22, thereby preventing a deformation of the lenses 22 when the lens stack is evacuated.

III.2 Array of 1-D convex lenses

[0093] In Fig. 9, a schematic plan view (Fig. 9(a)) and a schematic perspective view (Fig. 9(b)) of an array 36 of 1-D lenses is shown. The lens array 36 is comprised of three series arrangements 38a, 38b, 38c of lenses 40 that are arranged in series for being consecutively passed by a γ-beam. In the embodiment shown, N = 6 lenses 40 are arranged in series in each of the series arrangements 38a, 38b, 38c, however, the number N may in practice be much larger, i.e. $N \geq 10$, preferably $N \geq 100$ and more preferably $N \geq 300$, in order to increase the refractive power of the lens array 36.

[0094] As is further seen in Fig. 9, only M = 3 lens arrangements 38a, 38b, 38c are arranged in parallel in the lens array 36, but in practical applications, the number M could be much larger.

[0095] Each of the lenses 40 constituting the lens array 36 has two lens surfaces 42, 44 that have a convex shape in one dimension only. The convex shape can be seen in the plan view of Fig. 9(a), the shape having a tangential radius R at the apex of each lens surface 42, 44 of between 1 μm and 500 μm, preferably between 10 μ and 80 μm. This means that γ-beams 46 as shown in Fig. 9(a) will only be focused in the paper plane of Fig. 9(a), but not within a plane vertical to the paper plane of Fig. 9(a). Accordingly, when the lens array 36 of Fig. 9 is used alone, a γ-beam 46 would be focused onto a line rather than onto a focal point. However, in practice two lens arrays 36 could be arranged in series one after the other and rotated by 90° with respect to each other such as to achieve a focusing in two dimensions.

[0096] The use of lens surfaces 42, 44 that are convex only in one dimension is advantageous from a manufacturing point of view. The lens array 36 of Fig. 9 can be made from a wafer, such as an Si and/or Ge wafer by vertical etching, thereby leading to the vertical wall parts of the lens surfaces 42, 44. In particular, in producing the lens array 36, according to one embodiment first a mask is generated by electron beam lithography. Thereafter, the material between neighbouring lenses 40 is etched for example by ion beam deep etching. Preferably, the wafer thickness is between 20 μm and 100 μm and more preferably between 50 μm and 200 μm. With these thicknesses, precise vertical walls can still be etched.

[0097] Further, a plurality of identical lens arrays 36 as shown in Fig. 9 can be manufactured and then stacked one on top of the other to thereby increase the total thickness of the lens array 36. The wafers in the stack can be grown or fused together. This way, a total thickness of a lens array 36 of more than 5 mm or even more than 8 mm can be achieved.

III.3 Array of prisms

[0098] In Fig. 10(a) a plan view and in Fig. 10(b) a perspective view of an array 48 of triangular prisms 50 is shown.

The triangular prisms 50 have an isosceles triangle shape, wherein the height (h) of the triangle shape is smaller than 200 μm, preferably even smaller than 100 μm and more preferably even smaller than 50 μm, as miniaturizing again allows for increasing the number of prisms 50 to accommodate in the array and hence for increasing the total refractory power. The prisms 50 are also referred to as "wedges" or "microwedges" in the following.

[0099] Similar to the lens array 36 of Fig. 9, the wedge array 48 of Fig. 10 is likewise etched from a semiconductor wafer, in particular Si and/or Ge. Accordingly, the thickness of the wedges of Fig. 10 corresponds to the thickness of the wafer, which is again typically between 20 μm and 200 μm. As before, a plurality of identical wedge arrays 48 can be stacked on top of each other, to thereby produce a thicker wedge array 48 having a thickness of several millimetres or even beyond a centimeter.

[0100] Similar to the lens array 36 of Fig. 9, the wedge array 48 of Fig. 10 is also comprised of a number M of series arrangements 52a, 52b, 52c of wedges that are arranged in parallel, where the number M can again be chosen as desired. Further, each series arrangement 52a, 52b, 52c of wedges 50 contains a number N of wedges 50 arranged in series such as to be consecutively passed by a γ-beam. Herein, the number N will depend on the total deflection angle that is intended. From a manufacturing point of view, hundreds of or even a thousand wedges 50 can be easily provided in each arrangement of prisms 52a, 52b, 52c.

[0101] In Fig. 11, a combination of a lens array 36 of the kind shown in Fig. 9 and two wedge arrays 48 of the kind shown in Fig. 10 is schematically shown. As is seen in Fig. 11, since a plurality of series arrangements 36a to 36f are arranged in parallel, the lens array 36 can cover an incoming γ-beam 46 having a diameter that is much larger than the diameter of any individual lens 40. Accordingly, the plurality of series arrangements of lenses 36a to 36f separates the γ-beam 46 into a corresponding number of beamlets 54a to 54f and focuses the same. In the schematic representation of Fig. 11, each of the beamlets 54a to 54f is only focused in one dimension. However, by providing an additional lens array 36 rotated by 90° (not shown) with respect to the shown lens array 36, the beamlets 54a-f could as well be focused in two dimensions.

[0102] On the downstream side of the lens array 36, two wedge arrays 48 are shown, which deflect the individual beamlets 54a-f. For example, the wedge arrays 48 could be devised such as to focus individual beamlets 54a-f onto a line. For this, the angles of wedges 50 in different series arrangements of prisms 52a to 52c can be adjusted accordingly.

[0103] Accordingly, Fig. 11 demonstrates how the invention allows to focus a γ-beam having a comparatively large diameter onto a narrow line or a narrow spot using a plurality of microscopic optical elements, in particular small convex lenses 40 having very small radii of curvature and microwedges 50. With this, it is possible to focus γ-beams which may have a radius of a few 10 μm down to the nanometer or even femtometer range. This means that unprecedented γ-fluxes can be generated, which leads to many very promising applications, some of which are briefly described in section III.6 below.

III.4 Fresnel lenses and Fresnel zone plates

[0104] Fig. 12(a) and (b) show a plan view and a perspective view of a one-dimensional Fresnel lens 56. The general design is similar to what is known from light optics, although of course with a much smaller radius of curvature. In the Fresnel lens 56, the radius of curvature at the apex of the central zone 58 is smaller than 200 μm, preferably even smaller than 100 μm.

[0105] The Fresnel lens 56, similar to classical optics, seeks to avoid thick lenses with an excessive use of material and absorption by a step design. In the Fresnel lens 56 of Figs. 12(a) and (b), after a phase advance or 2π (defining a height $h = \frac{\lambda}{\delta}$), the shape of the lens is continued from the ground surface. With λ on the order of 10^{-12} m and δ on the order of 10^{-9}, the typical height h of the Fresnel lens 56 would be on the order of 1 mm.

[0106] Fig. 12(c) shows a similar design but for a 2-D-lens.

[0107] Fig. 13 shows a Fresnel zone plate having zones of at least two materials with different values of atomic number Z and atomic mass A, thus leading to a different phase advance δ. In the zone plate of Fig. 13, the central zone is a zone of larger phase advances δ (namely Au) as compared to the material of smaller phase advance, Si.

III.5 Monochromator

[0108] The novel refractive optical element for use with γ-photons described in the present invention can also be employed in combination with diffractive means. An important example of this combination is a novel monochromator that will be described with reference to Figs. 15 to 21. However, as a starting point of the explanation, the double crystal spectrometer 10 of Fig. 1 that has been used in the experimental measurement of the index of refraction for γ-beams is explained in more detail with reference to Fig. 14. Fig. 14 has been taken from E.G. Kessler et al., Nucl Inst. Meth. A 457, 187 (2001). Fig. 14 shows a schematic representation of a two-crystal spectrometer 10 having a first crystal 12

and a second crystal 14. The first and second crystals 12, 14 are referred to as "Laue-crystals" in the following, because they allow for a Laue-diffraction of the γ-beams at the crystal. The Laue-diffraction is the analogue of a Bragg-reflection except that the lattice planes involved in the diffraction are vertical with respect to the crystal surface onto which the radiation impinges rather than parallel to it, as is the case in Bragg-reflection. The angle satisfying the Laue-condition is therefore also often referred to as the Bragg-angle.

[0109] The left part of Fig. 14 shows the two-crystal spectrometer 10 in the non-dispersive geometry, in which the first and second Laue-crystals 12, 14 are parallel to each other. The portion of the incoming γ-beam that satisfies the Bragg-condition with regard to angle and wavelength, i.e. energy, is Laue-diffracted at the first Laue-crystal 12. The remainder of the beam that does not satisfy the Bragg-condition will simply be transmitted without diffraction by the first Laue-crystal 12 (undiffracted transmitted beam not shown in Fig. 14). Since in the non-dispersive geometry the first and second Laue-crystals 12, 14 are parallel, the crystal planes within the two crystals 12, 14 are parallel and consequently all wavelengths that are diffracted by the first Laue-crystal 12 will simultaneously satisfy the Bragg-condition at the second Laue-crystal 14 and will likewise be diffracted.

[0110] In the right part of Fig. 14, however, the second Laue-crystal 14 is inclined with regard to the first Laue-crystal 12 by twice the Bragg angle of a given wavelength λ. This means that at the second Laue-crystal 14, only photons with the corresponding wavelength λ will be Laue-diffracted. However, photons deviating from λ that have been Laue diffracted by the first Laue-crystal 12 do no longer meet the Bragg-condition at the second Laue-crystal 14 and will therefore be transmitted without diffraction by the second Laue-crystal 14 (undiffracted transmitted beam not shown). Accordingly, in the dispersive mode, the two-crystal spectrometer 10 acts as a monochromator, since the photons which are Laue-diffracted by the second Laue-crystal 14 are within a very narrow energy band.

[0111] However, when using the two-crystal spectrometer 10 in the dispersive geometry shown on the right hand side of Fig. 14, the efficiency, i.e. the fraction of photons of the original beam within a certain wavelength range $\lambda \pm \Delta\lambda$ that pass the monochromator, is strictly limited for the following reasons.

[0112] Within dynamical diffraction theory, it can be shown that for so-called perfect single crystals, the angle dependency of the intensity profile $I(\Theta)$ under which an incoming wave field is diffracted has the following analytical form

$$I(\Theta) = \frac{\sin^2(A\sqrt{1+y^2})}{1+y^2}$$

$$y \sim \frac{\Theta - \Theta_B}{\lambda}$$

[0113] Herein, A is a parameter that is linearly dependent on the wavelength and crystal thickness and further dependent on material and orientation specific parameters. From the above equation, it is easily demonstrated that the width of $I(\Theta)$ is proportional to λ meaning that the intensity-angle-profile $I(\Theta)$, which is also referred to as the "rocking curve", becomes very narrow for large energies. Example calculations of $I(\Theta)$ for a 2.5 mm thick single crystal of Si in [220] orientation are shown in Fig. 15 for photons of 100 keV, 500 keV and 1000 keV. As can be seen, the width of theses curves decreases with energy and can be as small as a few tens of nanoradiants (nrad).

[0114] The width of $I(\Theta)$ can be called the "acceptance with" of the single crystal, since it defines an angular range of photons of the given wavelength λ that will be "accepted" by the crystal in the sense that it is Laue-diffracted thereby. Conversely, this means that radiation impinging at an angle outside this acceptance range will not be Laue-diffracted by the first Laue-crystal 12, even if it has the desired energy (the appropriate wavelength λ) and will hence be lost for the monochromator of Fig. 14. Since the best collimated γ-beams typically have a divergence of the range of tens of microrad, this means that actually the biggest part of the impinging γ-beam will fall outside the angular acceptance range and hence be lost for the monochromator, thereby decreasing its efficiency.

[0115] Fig. 16 is a schematic representation of a monochromator 60 according to an embodiment of the present invention. The monochromator 60 comprises three pairs of Laue-crystals, 62a/62b, 64a/64a, 66a/66b which in combination each form a two-crystal spectrometer 10 in the dispersive geometry as shown on the right hand side of Fig. 14. All the first Laue-crystals 62a, 64a, 66a of all pairs of Laue-crystals 62a/62b, 64a/64a, 66a/66b are parallel to each other. Likewise, all the second Laue-crystals 62b, 64b, 66b of all pairs of Laue-crystals 62a/62b, 64a/64a, 66a/66b are parallel to each other. The first Laue-crystals 62a, 64a, 66a of the pairs of Laue-crystals 62a/62b, 64a/64a, 66a/66b are arranged in series with refractive deflection means 68 arranged inbetween neighbouring first Laue-crystals 62a, 64a, 66a such that the part of the beam that is transmitted without diffraction by one of the first Laue-crystals 62a, 64a is deflected prior to impinging on the next first Laue-crystal 64a, 66a in the series. While the refractive deflection means 68 is symbolically represented by a wedge prism 68 in Fig. 16, it is understood that in practice the wedge arrays as for example described

with reference to Figs. 10 and 12 above will be employed.

[0116] Next, the function of the monochromator 60 of Fig. 16 is explained with reference to Fig. 17. Panel A of Fig. 17 shows the intensity-angle profile of the incoming beam impinging on the first Laue-crystal 62a of the first pair of Laue-crystals 62a/62b. Only the portion of the beam that fulfils the Bragg-condition with respect to the first crystal 62a will be Laue-diffracted at the first Laue-crystal 62a. However, most of the beam will actually not meet the Bragg-condition and hence be transmitted without diffraction through the first crystal 62a of the first pair of Laue-crystals 62a/62b. This is indeed seen from panel B of Fig. 17, which shows the intensity-angle profile at location Ⓑ of Fig. 16, i.e. the intensity-angle profile of the beam that was transmitted without diffraction through the first Laue-crystal 62a. As is seen in panel B of Fig. 17, a small angular band of the intensity is missing, corresponding to the narrow angular band that has been Laue-diffracted by the first Laue-crystal 62a.

[0117] Next, the part of the beam transmitted without diffraction by the first Laue-crystal 62a passes the refractive deflection means 68. Panel C of Fig. 17 shows the intensity-angle profile at position Ⓒ just behind the refractive deflection means 68. As is seen from panel C of Fig. 17, the shape of the intensity-angle profile has not changed, but it has been shifted in angle space due to the refractive deflection means 68. Next, the beam with the shifted intensity-angle profile impinges onto the first Laue-crystal 64a of the second pair of Laue-crystals 64a/64b. Due to the angular shift of the intensity profile, the beam now contains a portion obeying the Bragg-condition with regard to angle and energy again, allowing for a further Laue-diffraction at the first Laue-crystal 64a of the second pair of Laue-crystals 64a/64b. Note in this regard that since all first Laue-crystals 62a, 64a, 66a of each pair of Laue-crystals 62a/62b, 64a/64b, 66a/66b are parallel to each other, the angular acceptance range for Laue-diffraction is always the same. However, due to deflection by the refractive deflection means 68, a portion of the beam energy that was outside the acceptance range of the previous first Laue-crystal (in this case 62a) and was hence transmitted without diffraction may now be shifted into the acceptance range and will be Laue-diffracted (in this case at 64a).

[0118] This is seen from panel D of Fig. 17, which shows the intensity-angle profile at location Ⓓ right behind the first Laue-crystal 64a of the second pair of Laue-crystals 64a/64b. As is seen from panel D of Fig. 17, a second angular band is missing in the intensity profile of the undiffracted transmitted beam, which corresponds to the portion of the beam that has been Laue-diffracted at the first Laue-crystal 64a of the second pair of Laue-crystals 64a/64b.

[0119] This procedure can be repeated with many pairs of Laue-crystals, where in each case the part of the beam that is transmitted without diffraction by the previous first Laue-crystal is deflected prior to impinging on the next first Laue-crystal in the series. Since only the Laue-diffracted portion of the beam adds to the output of the monochromator 60, it is seen that the efficiency of the monochromator 60 is thereby increased. When neglecting the losses within the multiple pairs of Laue-crystals and the refractive deflection means, the efficiency is generally proportional to the number of pairs of Laue-crystals. Herein, it is again advantageous that the absorption of γ-rays in matter is much less than in case of x-rays.

[0120] The efficiency increase is further illustrated with reference to Fig. 18 which schematically shows the energy and angular distribution of the γ-beam entering the monochromator 60. If only a single pair of Laue-crystals was used, only a small section of the angle-energy range of the impinging beam will be Laue-diffracted, which is schematically indicated by the small square 70 in Fig. 18. Namely, the small area 70 corresponds to the part of the angle-energy distribution that satisfies the Bragg-condition at the first Laue-crystal 62a, while the rest of the beam is transmitted without diffraction by the first Laue-crystal 62a and would be lost in an ordinary double-crystal spectrometer. However, by consecutively deflecting the beam transmitted without diffraction by the previous first Laue-crystal 62a, 64a, 66a, generally the full band 72 of desired energies can be consecutively harvested from the γ-beam, thereby increasing the efficiency of the monochromator 60.

[0121] Note that in the illustration of Fig. 16, the deflection of the beam by the refractive deflection means 68 has not been shown. The reason is that the angular shift of the intensity profile that is needed to "refill" the angular acceptance range is very small, since the angular acceptance range is very narrow. In principle, it is sufficient to provide for a shift that is slightly larger than the width of the acceptance range.

[0122] While the geometry of the monochromator 60 of Fig. 16 is particularly useful for explaining the inventive concept underlying the monochromator of the present invention, with regard to the practical implementation it is not the currently preferred embodiment. Note in this regard that the Bragg-angles of the Laue-diffraction have been illustrated extremely exaggerated in Fig. 16. In reality, the angular split between the undiffracted transmitted and the Laue-diffracted beams in practice is very small. Accordingly, while in Fig. 16 a beam that has already been Laue-diffracted by the first Laue-crystal, such as crystal 62a, avoids any further first Laue-crystal downstream thereof (such as Laue-crystal 64a), in view of the small angular separation between undiffracted transmitted and diffracted beams this may be difficult to achieve. Likewise, in the geometry of Fig. 16, the beam that is Laue-diffracted at the second Laue-crystal 62b of the first pair of Laue-crystals 62a/62b does not pass through the second Laue-crystal 64b of the second pair of Laue-crystals 64a/64b. However, if this was the case, then the beam diffracted by the second Laue-crystal 62b would be Laue-diffracted at the second Laue-crystal 64b again, which is not desired. Instead, it is intended that in the monochromator 60, each beam of the desired energy is Laue-diffracted exactly once at a first Laue-crystal 62a, 64a, 66a and once at a corresponding

second Laue-crystal 62b, 64b, 66b. This can indeed be achieved even if the Laue-diffracted beam passes through multiple further Laue-crystals of the same kind, if it is ensured that a beam that has already been Laue-diffracted by a first (second) Laue-crystal of one pair of Laue-crystals is deflected using refractive deflection means prior to passing a first (second) Laue-crystal of another pair of Laue-crystals. Namely, due to the angle change in the deflection, the already diffracted beam does no longer obey the Bragg-condition if passing a Laue-crystal of the same kind (first or second) later on and hence will not be Laue-diffracted again.

[0123] An example of such an arrangement is shown in the monochromator 74 of Fig. 19. In Fig. 19, again three pairs of Laue-crystals 62a/62b, 64a/64b, 66a/66b and refractive deflection means 68 are shown. In the embodiment of Fig. 19, all first Laue-crystals 62a, 64a, 66a are part of a (fixed) first unit 76 that is made from a single crystal block. Likewise, all second Laue-crystals 62b, 64b and 66b are part of one fixed second unit 78 and are also made from a single crystal block. This way, it is ensured that all first Laue-crystals 62a, 64a, 66a and all second Laue-crystals 62b, 64b, 66b are parallel with each other, respectively. Preferably, both units 76 and 78 are taken from the same ingot, so that the lattice structures ideally match.

[0124] In the monochromator 74 of Fig. 19, the refractive deflection means 68 arranged between two adjacent first Laue-crystals 62a/64a, 64a/66a for deflecting a beam transmitted without diffraction by the previous first Laue-crystals 62a, 64a in the series is arranged to also deflect the beam that is Laue-diffracted by the previous first Laue-crystal 62a, 64a. This way, it is avoided that a beam that has been Laue-diffracted at one of the first Laue-crystals 62a, 64a is diffracted at another first Laue-crystal 64a, 66a in the monochromator 74 again. Likewise, the geometry of the monochromator 74 ensures that a beam that has been Laue-diffracted at one of the second Laue-crystals 62b, 64b is deflected once before passing another second Laue-crystal 64b, 66b, thereby avoiding a further Laue-diffraction at a second Laue-crystal.

[0125] Note that in the monochromator 74 of Fig. 19, the tilt angle between the first Laue-crystals 62a, 64a, 66a and the second Laue-crystals 62b, 64b, 66b does not correspond to twice the Bragg-angle, since the angular shift of the refractive deflection means 68 needs to be taken into account.

[0126] Further, note that the beams that are Laue-diffracted at the plural second Laue-crystals 62b, 64b, 66b diverge when leaving the monochromator 74, since they have passed different numbers of refractive deflection means 68. However, these individual beams extracted from the monochromator 74 can be focused to a single spot using an appropriate lens system.

[0127] In Fig. 20, yet a further monochromator 80 is shown, which has the currently most preferred geometry. The monochromator 80 also comprises two units 76, 78, where the first unit 76 contains three first Laue-crystals 62a, 64a, 66a and the second unit 78 contains three second Laue-crystals 62b, 64b, 66b. Note that in the monochromator 80, the first and second units 76, 78 are arranged in series, while in the monochromator 74 of Fig. 19, they were arranged in an interleaved relationship. That is to say, in the monochromator 80 of Fig. 20, all first Laue-crystals 62a, 64a, 66a are arranged in a series and all second Laue-crystals 62b, 64b, 66b are arranged in a further series that is arranged downstream of the series of first Laue-crystals 62a, 64a, 66a with regard to the propagation direction of the beam. Also, from a functional point of view, the order of the second crystals 62b, 64b, 66b in the second unit 78 is reversed in the sense that the most upstream first Laue-crystal 62a of the first unit 76 forms a Laue-crystal pair with the most downstream second crystal 62b of the second unit 78 and so on.

[0128] Refractive deflection means 68 are placed between each two neighbouring first Laue-crystals 62a, 64a, 66a of the first unit 76 in order to provide for the desired angular shift. Further refractive deflection means 82 are placed between each two neighbouring second Laue-crystals 62b, 64b, 66b of the second unit 78. Herein, the further refractive deflection means 82 compensate the effects of the refractive deflection means 68 arranged in the first unit 76. For example, the refractive deflection means 68 and 82 could be identical wedge arrays similar to those shown in Fig. 10 but with reversed orientation, as is symbolically shown in Fig. 20

[0129] However, it is not necessary that all the refractive deflection means 68, 82 in the gaps between adjacent Laue-crystals are identical. Instead, it is sufficient that the reflection means 82 in the n^{th} gap between neighbouring second Laue-crystals 62b, 64b, 66b when counted in opposite propagation direction of the beam is adapted to compensate for the deflection provided by the deflection means 68 in the n^{th} gap between neighbouring first Laue-crystals 62a, 64a, 66a when counted in propagation direction of the beam.

[0130] Note that with the geometry of Fig. 20, generally all undiffracted transmitted or diffracted beams may pass through all Laue-crystals 62 a/b, 64a/b, 66a/b of both units 76, 78 and all refractive deflection means 68, 82, while still ensuring that each beam portion of the desired energy is only Laue-diffracted by exactly one pair of the first and second Laue-crystals 62a/b, 64a/b, 66a/b.

[0131] The efficiency of each of the monochromators 60, 74 and 80 is further increased if the inherently diverging beam is made less diverging or even parallelized prior to entering the monochromator 60, 74, 80. For this, the collimation lenses, lens stacks or lens arrays discussed above with reference to Figs. 8, 9, 12 and 13 can be ideally used. Note in this regard that a focusing lens acts as a collimation lens if the source of the diverging beam is placed in the focal point of the lens.

[0132] In Fig. 21, a schematic perspective view of a Laue-crystal unit 84 is shown, that could be used as one of the units 76 or 78 of Fig. 20. The unit shows three Laue-crystals 62, 64, 66 which are made from one ingot. Further shown are the refractive deflection means 68, which are formed by wedge arrays 68 in the present example. Note that Fig. 21 is also highly schematic and not drawn to scale. Further, the wedge arrays 68 can be adjusted with respect to each other by means of a flexure cut 86 and a piezo actuator 88. By controlling the piezo actuator 88, the relative orientation of the wedge arrays 68 can therefore be adjusted such as to tune the monochromator 80.

[0133] The monochromator 80 of Fig. 20 is particularly useful in that it allows not only generating a highly monochromatic γ-beam with a comparatively high efficiency, but at the same time parallelizing the outputted γ-beam.

III.6 Applications

[0134] As is apparent from the above description, the present invention provides various refractive optical means for shaping, deflecting or monochromatizing a beam of γ-photons. This will find many useful applications, some of which are briefly discussed below.

[0135] In particular, with the lens arrays of convex γ-lenses, beams can be collimated or focused. Accordingly, it is possible to focus γ-beams having a diameter of a few 10 μm to the submicrometer or even subnanometer regime, leading to a flux increase of 10^6 or more, possibly even up to 10^{10}. Such high fluxes are for example important when small targets of expensive separated and/or enriched isotopes are used to efficiently produce radioisotopes for medical applications as is explained in further detail in *D. Habs and U. Köster, Appl. Phys. B 103, 501 (2011).*

[0136] A further use for γ-beams with highly increased flux is the excitation of neutron-halo isomers at γ-energies close to the neutron binding energy of typically 7 to 8 MeV, which corresponds to the region of the so-called pygmy resonance. For these halo-isomers, a second short wavelength laser can release cold neutrons resulting in a very brilliant micro neutron beam, see D. Habs et al., App. Phys. B 103 485 (2011*).* Herein, the flux increase by focusing the γ-beam would result in an equivalent strong increase of the brilliance of the neutron beam. Furthermore, neutron beams with small diameter (μm, nm or even fm) would become available.

[0137] Further, for the production of moderated positron beams it is essential to have a very small diameter γ-beam, because then the converter foils of high Z material (W or Pt) can have much smaller heights. This way, the distance between the high Z-foils can be reduced correspondingly, and a more compact and more efficient system becomes possible, see C. Hugenschmidt et al., Appl. Phys. B , DOI 10.1007/s00340-011-4594-0 (2011*).*

[0138] These are only some of the many examples where focusing leads to much more brilliant secondary sources.

[0139] While x-rays generally address the electrons of the atomic shell, γ-beams can be used to address the nuclear isotopes. The advantage of γ-beams is that they are much more penetrating than x-rays but still have very large selective cross sections when resonance is met. Accordingly, within large containments, specific isotopes can be addressed with matched γ-optics without destructive sample preparation. The detection of the resonance can be done for example with nuclear resonance fluorescence (NRF) techniques and/or secondary triggered nuclear reactions, such as β- or α-decays. For this reason, γ-beams can be ideally used in microscopy and tomography applications by tuning the γ-energy to nuclear resonances. Then, by turning the object in the γ-beam, a tomographic picture can be obtained. With the new monochromator disclosed herein, the resonance can be very exactly matched. Using γ-tomography, one can for example examine radioactive waste without having to open the containment, e.g. by looking for absorption in the beam by NRF. With γ-tomography methods, one can also study complex systems like airplane engines, car batteries, burning rods or nuclear reactors (while under operation) or the like. However, tomography can also be used to examine medical patients with high isotope selectivity from larger distance.

[0140] When focusing a primary incoherent γ-beam to very small spot sizes, the γ-beam becomes laterally partially coherent, see e.g. C.G. Schroer et al., Phys. Rev. Let. 1001, 090801 (2008*).* There is currently a rapid development in coherent x-ray optics, see for example D.M. Paganin, Coherent X-Ray Optics , Oxford University Press, Oxford, United Kingdom (2006) and further references therein. Using the refractive γ-optics elements of the invention, the developments from the x-ray regime can be carried over to the γ-regime. For example, the present inventors are currently working on a project to produce the first γ-FEL (free electron laser) which is expected to lead to even more brilliant γ-beams. Herein, a seeding of the electron laser interacting with a partially coherent γ-beam is essential, which becomes possible with the new focusing system described herein.

[0141] The embodiments described above and the accompanying figures merely serve to illustrate the method according to the present invention, and should not be taken to indicate any limitation of the method. The scope of the patent is solely determined by the following claims.

Claims

1. The use of one or more refractive optical elements for one or more of

- shaping,
- deflecting, and
- guiding by total internal reflection

a beam of γ-photons having an energy for which the energy dependent index of refraction of the material of said refractive optical element has a real part that is larger than 1.

2. The use of one or more refractive optical elements of claim 1, wherein the energy of the γ-photons is larger than 100 keV, preferably larger than 300 keV, more preferably larger than 500 keV, larger than 700 keV and larger than 1 MeV,and/or wherein said shaping of said γ-beam comprises one or more of the following:

- focussing said γ-beam at least in one dimension,
- collimating said γ-beam at least in one dimension,
- diverging said γ-beam at least in one dimension, and
- separating a γ-beam into individual beamlets, in particular into parallel beamlets and/or wherein the γ-beam is provided by Compton back-scattering of laser light from an electron beam.

3. The use of claim 3, wherein the γ-beam is focused or collimated using a convex lens (22) or a plurality of convex lenses arranged in series, each convex lens (22) having at least one, preferably two lens surfaces (24, 26) having a shape that is convex in at least one dimension,
wherein said convex lens (22) preferably has at least one, preferably two lens surfaces (24, 26) having a convex shape in two dimensions, and in particular, a rotation-ellipsoid shape,
wherein said convex lens (22) is preferably made from an embossed foil, in particular a foil comprising one of Be, Al, Ni, Ta or Th as its main constituents, or by micromachining,
wherein preferably the tangential radius R at the apex of the lens is < 2000 μm, preferably < 1000 μm and preferably between 5 μm and 500 μm, and/or
wherein preferably a number N of said convex lenses (22) are arranged in series, in particular stacked one behind the other in a lens holder, wherein N is between 2 and 10000,
preferably between 10 and 200,
wherein the body of said lens (22) preferably has a hole (34) for ventilation.

4. The use of claim 2, wherein said γ-beam is focused or collimated by an array (36) of lenses (40),
said array (36) of lenses (40) comprising at least one series arrangement (38a, 38b, 3 8c) of lenses (40) allowing for being consecutively passed by a γ-beam, wherein at least the majority of the lenses (40) has at least one, preferably two lens surfaces (42, 44) having a convex shape in at least one dimension
wherein preferably the mean radius of curvature of the convex shape or the tangential radius at the apex of the convex shape is between 1 μm and 500 μm, preferably between 10 μm and 80 μm, and/or
wherein in said series arrangement (38a, 38b, 38c), a number N of lenses are arranged in series such as to be consecutively passed by a γ-beam, wherein $N \geq 10$, preferably $N \geq 100$, and more preferably $N \geq 300$, and/or
wherein said array (36) of lenses (40) comprises a number M of series arrangements (38a, 38b, 38c) of lenses arranged in parallel,
wherein $M \geq 2$, preferably $M \geq 4$, and more preferably $M \geq 10$, and/or
wherein said lens array (36) is at least in part made from one or more wafers, in particular Si- and/or Ge-wafers, in which the lens surfaces (42, 44) are formed by etching,
wherein in particular said one or more wafers has/have a thickness between 20 μm and 200 μm, preferably between 50 μm and 100 μm, and/or
wherein said lens array (36) is at least in part made from a stack of a plurality of identically etched wafers,
wherein said wafers of said stack are preferably grown or fused together and/or wherein
the total thickness of the stack of wafers is preferably 5 mm or more, more preferably 8 mm or more, and/or
wherein said γ-beam is focused or collimated by two arrays (36) of lenses (40), according to one of the above embodiments and arranged in series, wherein the arrays are oriented with respect to each other, such that each of the two lens arrays (36) focuses or collimates a γ-beam within a different plane, wherein said planes are preferably arranged at 90° with respect to each other.

5. The use of claim 1 or 2, wherein said γ-beam is deflected by an array (48) of prisms (50),
said array (48) of prisms (50) comprising at least one series arrangement (52a, 52b, 52c) of prisms (50) allowing for being consecutively passed by a γ-beam,

wherein in said series arrangement (52a, 52b, 52c) of prisms (50), preferably a number N of prisms are arranged in series, such as to be consecutively passed by a γ-beam,
wherein $N \geq 2$, preferably $N \geq 10$ and more preferably $N \geq 100$, and/or
wherein at least the majority of prisms (50) in said array (48) of prisms has a wedge shape with a base surface having a triangular shape,
wherein the height (h) of the triangular shape is smaller than 200 μm, preferably smaller than 50 μm,
wherein the base surface preferably has an isosceles triangle shape,
wherein the angle γ between the two equal sides of said isosceles triangle is preferably between 5° and 120°, more preferably between 15° and 90°, and/or
wherein said array (48) of prisms (50) comprises a number M of series arrangements (52a, 52b, 52c) of prisms arranged in parallel,
wherein $M \geq 2$, preferably $M \geq 4$ and more preferably $M \geq 10$, and/or
wherein said array (48) of prisms (50) is at least in part made from one or more wafers,
in particular Si and/or Ge wafers, in which the prisms (50) are formed by etching,
wherein said one or more wafers preferably has/have a thickness between 20 μm and 200 μm, preferably between 50 μm and 100 μm, and/or
wherein said array (48) of prisms (50) is at least in part made from a stack of a plurality of identically etched wafers,
wherein said wafers of said stack are preferably grown or fused together, and/or
wherein the total thickness of the stack of wafers is preferably 5 mm or more, more preferably 8 mm or more.

6. The use of claim 2, wherein said one or more refractive optical element comprises a lens array (36) according to claim 4, configured for separating a γ-beam (46) into individual beamlets (54a-f) and focusing the individual beamlets (54a-f) by means of said series arrangements (38a-f) of lenses (40) arranged in parallel, and a prism array (48) according to one of claims 20 to 23, arranged such as to receive and deflect the individual beamlets (54a-f), wherein the array (48) of prisms (50) is in particular adapted to converge the individual beamlets (54a-f) at a common focal point or focal area.

7. The use of one of the preceding claims, wherein the γ-beam is shaped using a one-dimensional or two-dimensional Fresnel lens (56),
wherein the γ-beam is preferably focused or collimated using a Fresnel lens (56) having a convex shape in its central zone (58), wherein the mean radius of curvature in the central zone (58) or at the apex of the central zone is preferably between 1 μm and 200 μm,
and/or
wherein the γ-beam is shaped using a Fresnel zone plate having zones of at least two materials with different values of atomic number Z and atomic mass A, thus leading to a different phase advance δ, wherein the γ-beam is preferably focused or collimated using said Fresnel zone plate, wherein the central zone is a zone of larger phase advance δ.

8. The use of one of the preceding claims, wherein the one or more refractive optical elements are employed in a monochromator (60, 74, 80) for monochromatizing a beam of γ-photons,
said monochromator comprising a plurality of pairs of Laue-crystals, each pair of Laue-crystals (62a/b, 64a/b, 66a/b) having

- a first Laue-crystal (62a, 64a, 66a) for diffracting a portion of an incoming beam that meets the Bragg-condition and transmitting the remainder of the incoming beam, and
- a second Laue-crystal (62b, 64b, 66b) arranged with respect to the first Laue-crystal (62a, 64a, 66a) such as to allow for a further Laue diffraction of the beam portion that was Laue-diffracted at the first Laue-crystal (62a, 64a, 66a) of said pair of Laue-crystals,

wherein the first Laue-crystals (62a, 64a, 66a) of all pairs of Laue-crystals are parallel to each other and the second Laue-crystals (62b, 64b, 66b) of all pairs of Laue-crystals are parallel to each other, and
wherein the first Laue-crystals (62a, 64a, 66a) of the pairs of Laue-crystals are arranged in series with refractive deflection means (68) arranged inbetween such that the part of the beam that is transmitted by one of said first Laue-crystals (62a, 64a) is deflected prior to impinging on the next first Laue-crystal (64a, 66a) in said series.

9. The use of claim 8, wherein the refractive deflection means arranged between consecutive first Laue-crystals (62a, 64a, 66a) in said series of first Laue-crystals are adapted to deflect the beam by an angle α, with 5 nrad < α < 200 nrad, preferably 10 nrad < α < 100 nrad, and/or
wherein the number of pairs of Laue-crystals (62a/b, 64a/b, 66a/b) is at least 5, preferably at least 10 and more

preferably at least 50, and/or
wherein the first and second Laue-crystals (62a/b, 64a/b, 66a/b) of each pair of Laue-crystals are either

- parallel to each other, or
- inclined with respect to each other such as to allow for an energy selection by two consecutive Laue-diffractions, and in particular inclined by twice of a Bragg-angle of the desired wavelength, or
- shiftable between the two configurations,and/or

wherein all first Laue-crystals (62a, 64a, 66a) are part of one fixed first unit (76) and all second Laue-crystals (62b, 64b, 66b) are part of one fixed second unit (78),
wherein the first and second units (76, 78) are preferably each made from a single crystal block in particular an Si or Ge block, wherein both blocks are preferably taken from the same ingot, and/or
wherein a collimating lens, lens stack or lens array is arranged upstream of the monochromator (60, 74, 80) such as to parallelize or at least reduce the divergence of the beam prior to entering the monochromator (60, 74, 80),
wherein the collimating lens, lens stack or lens array is preferably of one of the kinds defined in one of claims 3 to 4, and/or
wherein a beam that has already been Laue-diffracted by a first (second) Laue-crystal of one pair is deflected using a refractive deflection means (68) prior to passing a first (second) Laue-crystal of another pair of Laue-crystals,
wherein the refractive deflection means (68) arranged between two adjacent first Laue-crystals (62a, 64a, 66a) for deflecting a beam transmitted by the previous first Laue-crystal (62a, 64a) in said series is arranged to also deflect the beam Laue-diffracted by said previous first Laue-crystal,
and/or
wherein the first and second Laue-crystals (62a/b, 64a/b, 66a/b) are arranged in the monochromator (74) such that the first and second Laue-crystals (62a/b, 64a/b, 66a/b) of each pair are adjacent to each other, or
wherein the first and second Laue-crystals (62a/b, 64a/b, 66a/b) are arranged in the monochromator (80) such that all first Laue-crystals (62a, 64a, 66a) are arranged in a series and all second Laue-crystals (62b, 64b, 66b) are arranged in a further series that is arranged downstream of the series of first Laue-crystals (62a, 64a, 66a),
wherein first refractive deflecting means (68) are placed between each two neighbouring first Laue-crystals (62a, 64a, 66a) and second refractive deflecting means (82) are placed between each two neighbouring second Laue-crystals (62b, 64b, 66b) with regard to the propagation direction of the beam,
wherein the second refractive deflection means (82) in the n^{th} gap between neighbouring second Laue-crystals (62b, 64b, 66b) when counted in opposite propagation direction of the beam is adapted to compensate for the deflection provided by the first refractive deflection means (68) in the n^{th} gap between neighbouring first Laue-crystals (62a, 64a, 66a) when counted in propagation direction of the beam.

10. A focusing lens (22) for focusing a beam of γ-photons,
wherein the focusing lens (22) is a convex lens having at least one, preferably two lens surfaces (24, 26) having a convex shape in two dimensions, and in particular, a rotation-ellipsoid shape,
wherein the tangential radius R at the apex of the lens is < 2000 μm, preferably < 1000 μm and preferably between 5 μm and 500 μm,
wherein said focusing lens (22) is preferably made from an embossed foil, in particular a foil comprising one of Be, Al, Ni, Ta or Th as its main constituents, or
a stack of N such focusing lenses (22) arranged in series, in particular stacked one behind the other in a lens holder, wherein N is between 2 and 10000, preferably between 10 and 200.

11. A lens array (36) for focusing a beam of γ-photons, said lens array (36) comprising at least one series arrangement (38a, 38b, 38c) of lenses (40) allowing for being consecutively passed by a γ-beam, wherein at least the majority of the lenses (40) has at least one, preferably two lens surfaces (42, 44) having a convex shape in at least one dimension,
wherein the mean radius of curvature of the convex shape or the tangential radius at the apex of the convex shape is preferably between 1 μm and 500 μm, preferably between 10 μm and 80 μm,
wherein in said series arrangement (38a, 38b, 38c), preferably a number N of lenses are arranged in series such as to be consecutively passed by a γ-beam, wherein $N \geq 10$,
preferably $N \geq 100$, and more preferably $N \geq 300$, and/or
wherein said lens array (36) comprises a number M of series arrangements (38a, 38b, 38c) of lenses (40) arranged in parallel,
wherein $M \geq 2$, preferably $M \geq 4$, and more preferably $M \geq 10$, and/or
wherein said lens array (36) is at least in part made from one or more wafers, in particular Si- and/or Ge-wafers, in

which the lens surfaces are formed by etching, wherein said one or more wafers preferably has/have a thickness between 20 μm and 200 μm, preferably between 50 μm and 100 μm, and/or
wherein said lens array is at least in part made from a stack of a plurality of identically etched wafers,
wherein said wafers of said stack are preferably grown or fused together and/or wherein the total thickness of the stack of wafers is preferably 5 mm or more, more preferably 8 mm or more.

12. A combination of two lens arrays (36) , each according to claim 11 and arranged in series, wherein the arrays (36) are oriented with respect to each other, such that each of the two lens arrays (36) focuses or collimates a γ-beam within a different plane, wherein said planes are preferably arranged at 90° with respect to each other.

13. A Fresnel lens (56) for focusing a beam of γ-photons, said Fresnel lens (56) having a convex shape in its central zone (58), wherein the mean radius of curvature in the central zone (58) or at the apex of the central zone (58) is preferably between 5 μm and 200 μm, or
a Fresnel zone plate for focusing a beam of γ-photons, said Fresnel zone plate having zones of at least two different indices of refraction.

14. A monochromator (60, 74, 80) for monochromatizing a beam of γ-photons,
said monochromator comprising a plurality of pairs of Laue-crystals (62a/b, 64a/b, 66a/b), each pair of Laue-crystals having

- a first Laue-crystal (62a, 64a, 66a) for diffracting a portion of an incoming beam that meets the Bragg-condition and transmitting the remainder of the incoming beam without diffraction, and
- a second Laue-crystal (62b, 64b, 66b) arranged with respect to the first Laue-crystal (62a, 64a, 66a) such as to allow for a further Laue diffraction of the beam portion that was Laue-diffracted at the first Laue-crystal (62a, 64a, 66a) of said pair of Laue-crystals (62a/b, 64a/b,66a/b),

wherein the first Laue-crystals (62a, 64a, 66a) of all pairs of Laue-crystals (62a/b, 64a/b,66a/b) are parallel to each other and the second Laue-crystals (62b, 64b, 66b) of all pairs of Laue-crystals (62a/b, 64a/b,66a/b)are parallel to each other, and
wherein the first Laue-crystals (62a, 64a, 66a) of the pairs of Laue-crystals (62a/b, 64a/b,66a/b) are arranged in series with refractive deflection means (68) arranged inbetween such that the part of the beam that is transmitted without diffraction by one of said first Laue-crystals (62a, 64a) is deflected prior to impinging on the next first Laue-crystal (64a, 66a) in said series.

15. The monochromator (60, 74, 80) of claim 14, wherein the refractive deflection means (68) arranged between consecutive first Laue-crystals (62a, 64a, 66a) in said series of first Laue-crystals are adapted to deflect the beam by an angle α, with $5 < \alpha < 200$ nrad, preferably $10 < \alpha < 100$ nrad, and/or
wherein the number of pairs of Laue-crystals (62a/b, 64a/b, 66a/b) is at least 5, preferably at least 10 and more preferably at least 50, and/or
wherein the first and second Laue-crystals (62a/b, 64a/b, 66a/b) of each pair of Laue-crystals (62a/b, 64a/b,66a/b) are either

- parallel to each other, or
- inclined with respect to each other such as to allow for an energy selection by two consecutive Laue-diffractions, in particular inclined by twice a Bragg-angle of the desired wavelength, or
- shiftable between the two configurations, and/or

wherein all first Laue-crystals (62a, 64a, 66a) are part of one fixed first unit (76) and all second Laue-crystals (62b, 64b, 66b) are part of one fixed second unit (78),
wherein the first and second units (76, 78) are preferably each made from a single crystal block, in particular an Si or Ge block, wherein both blocks are preferably taken from the same ingot, and/or
wherein a collimating lens, lens stack or lens array is arranged upstream of the monochromator (60, 74, 80) such as to parallelize or at least reduce the divergence of the beam prior to entering the monochromator (60, 74, 80), wherein the collimating lens, lens stack or lens array is preferably a lens, lens stack or lens array according to one of claims 10 to 13, and/or
wherein a beam that has already been Laue-diffracted by a first (second) Laue-crystal of one pair is deflected using a refractive deflection means (68) prior to passing a first (second) Laue-crystal of another pair of Laue-crystals, and/or
wherein the refractive deflection means (68) arranged between two adjacent first Laue-crystals (62a, 64a, 66a) for

deflecting a beam transmitted without diffraction by the previous first Laue-crystal (62a, 64a) in said series is arranged to also deflect the beam Laue-reflected by said previous first Laue-crystal (62a, 64a), and/or
wherein the first and second Laue-crystals (62a/b, 64a/b, 66a/b) are arranged in the monochromator (74) such that the first and second Laue-crystals of each pair are adjacent to each other, or
wherein the first and second Laue-crystals (62a/b, 64a/b, 66a/b) are arranged in the monochromator such that all first Laue-crystals (62a, 64a, 66a) are arranged in a series and all second Laue-crystals (62b, 64b, 66b) are arranged in a further series that is arranged downstream of the series of first Laue-crystals (62a, 64a, 66a),
wherein first refractive deflection means (68) are placed between each two neighbouring first Laue-crystals (62a, 64a, 66a) and second refractive deflection means (82) are placed between each two neighbouring second Laue-crystals (62b, 64b, 66b) with regard to the propagation direction of the beam,
wherein the second refractive deflection means (82) in the n^{th} gap between neighbouring second Laue-crystals (62b, 64b, 66b) when counted in opposite propagation direction of the beam is adapted to compensate for the deflection provided by the first refractive deflection means (68) in the n^{th} gap between neighbouring first Laue-crystals (62a, 64a, 66a) when counted in propagation direction of the beam.

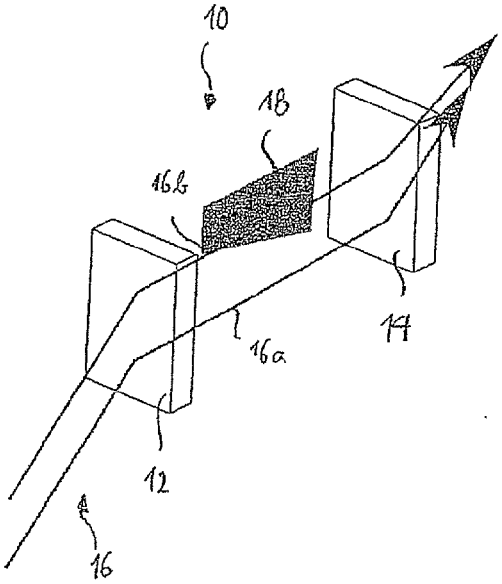
10
18
16b
16a
14
12
16

Fig. 1

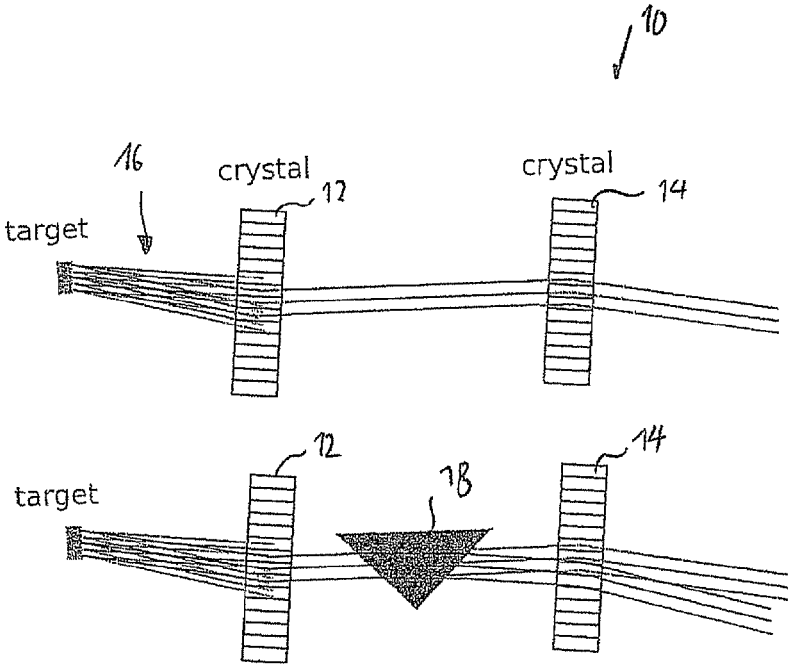
10
16
target
crystal
12
crystal
14
target
12
18
14

Fig. 2

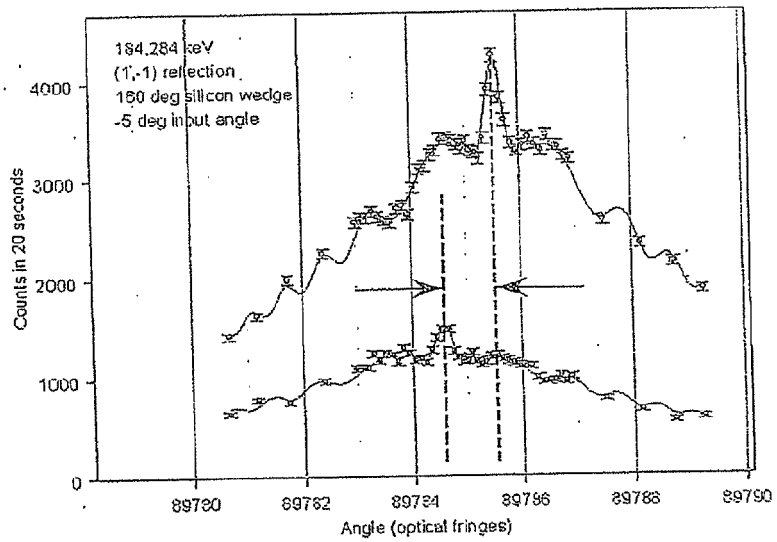

Fig. 3

γ energy keV	δ	γ energy keV	δ
	^{36}Cl		$^{156,158}Gd$
517.1	$(-4.63 \pm 1.75) \cdot 10^{-10}$	181.9	$(-1.11 \pm 0.07) \cdot 10^{-8}$
786.3	$(+1.83 \pm 1.57) \cdot 10^{-10}$	606.4	$(-7.91 \pm 8.00) \cdot 10^{-10}$
1164.9	$(+1.48 \pm 0.13) \cdot 10^{-9}$	780.2	$(-1.48 \pm 0.48) \cdot 10^{-9}$
1951.2	$(+1.11 \pm 0.30) \cdot 10^{-9}$	897.5	$(+2.96 \pm 5.17) \cdot 10^{-10}$
		944.2	$(+4.09 \pm 3.26) \cdot 10^{-10}$

Fig. 4

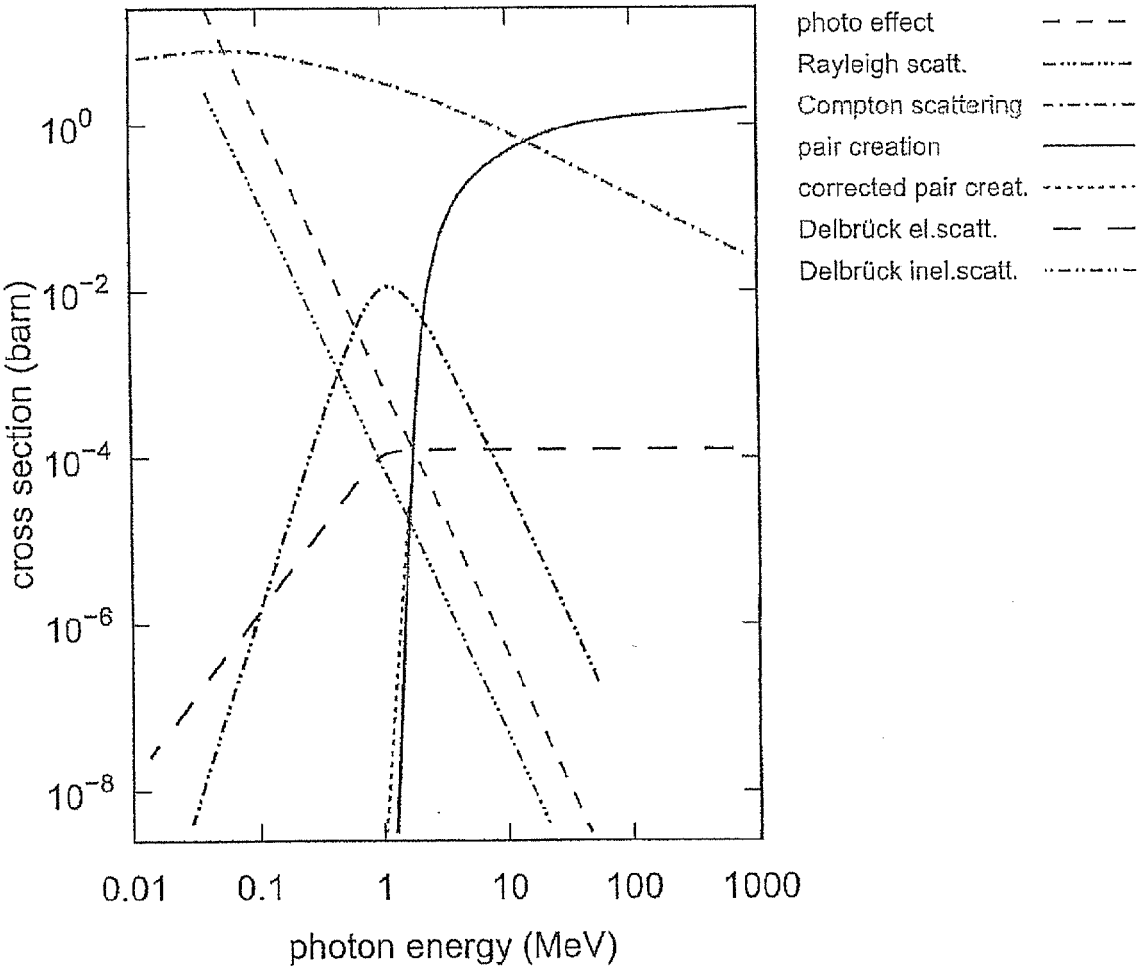
photo effect
Rayleigh scatt.
Compton scattering
pair creation
corrected pair creat.
Delbrück el.scatt.
Delbrück inel.scatt.
cross section (barn)
10^{0}
10^{-2}
10^{-4}
10^{-6}
10^{-8}
0.01
0.1
1
10
100
1000
photon energy (MeV)

Fig. 5

Fig. 6

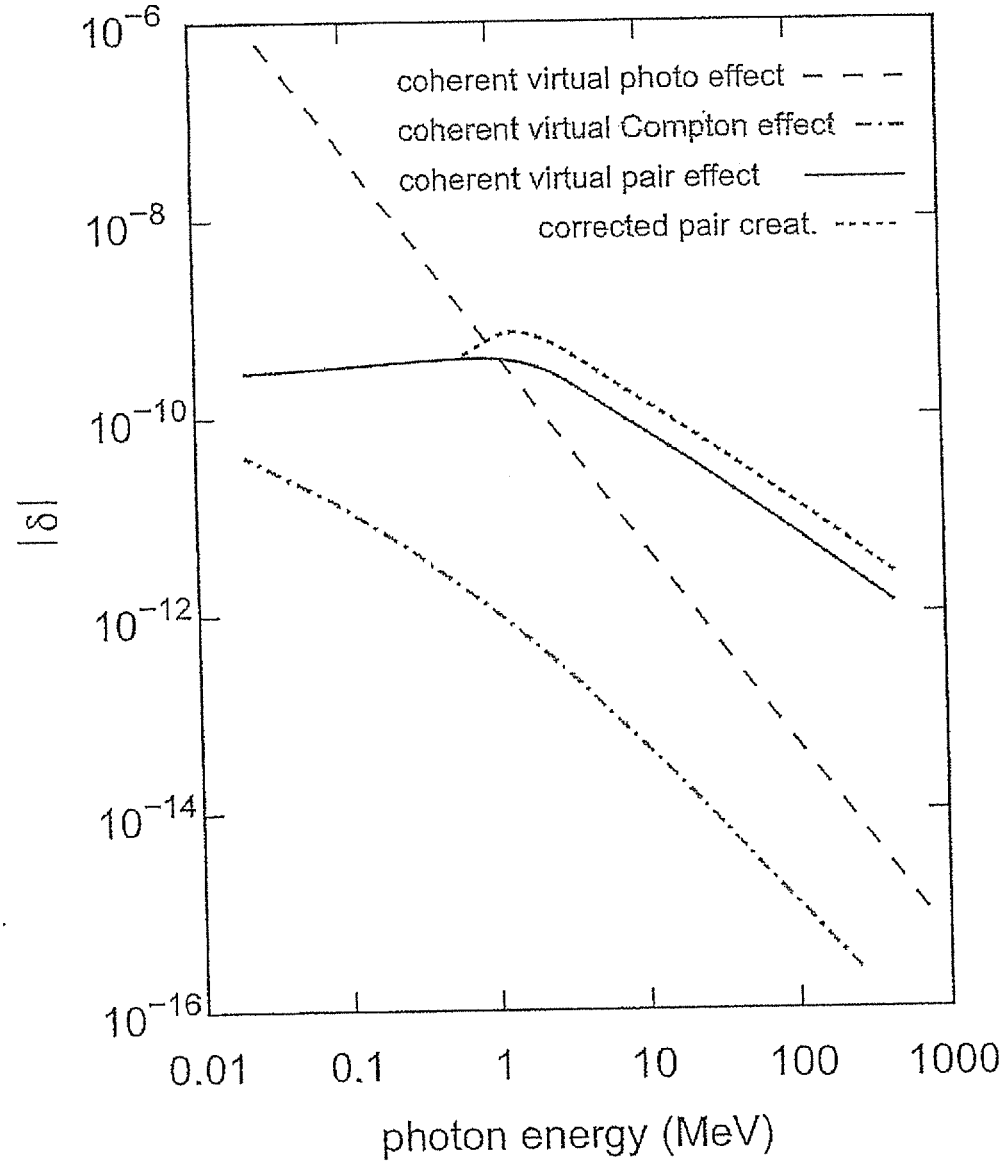
coherent virtual photo effect
coherent virtual Compton effect
coherent virtual pair effect
corrected pair creat.
10^{-6}
10^{-8}
10^{-10}
10^{-12}
10^{-14}
10^{-16}
|δ|
0.01
0.1
1
10
100
1000
photon energy (MeV)

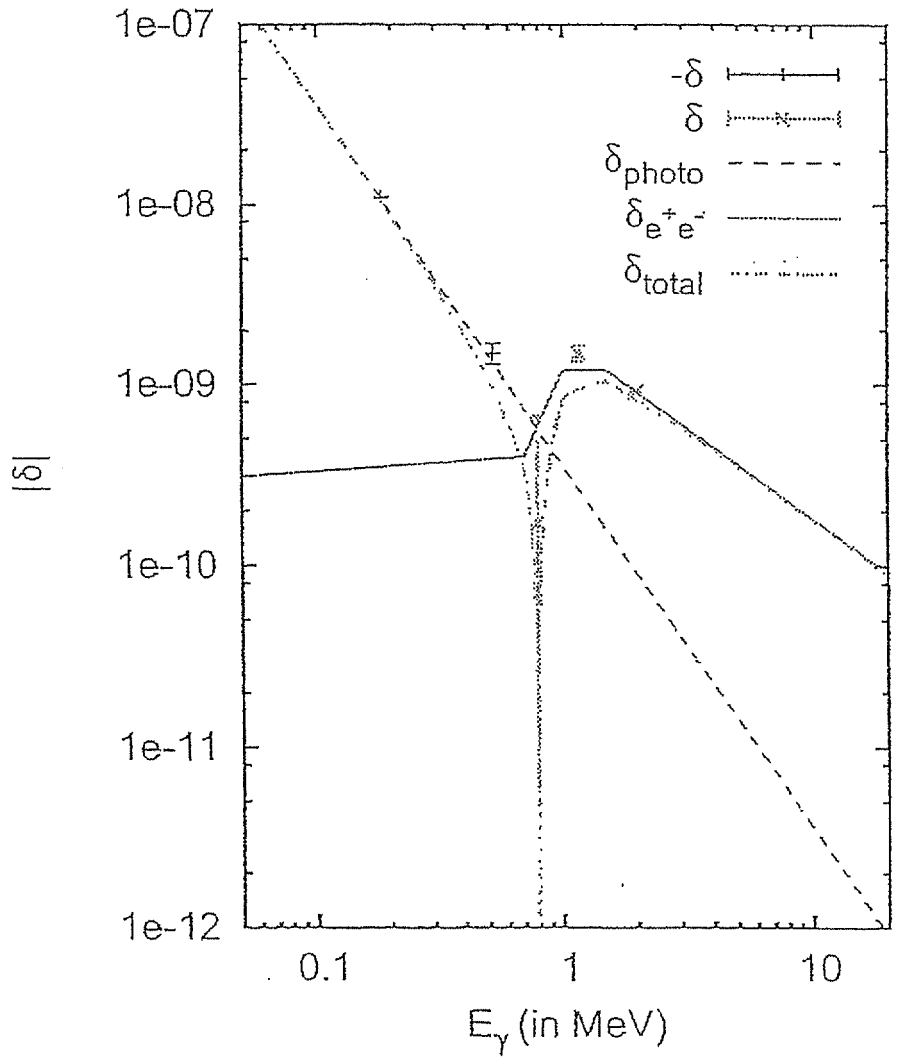
1e-07
1e-08
1e-09
1e-10
1e-11
1e-12
|δ|
0.1
1
10
E_γ (in MeV)
-δ
δ
δ_photo
δ_e+e-
δ_total

Fig. 7

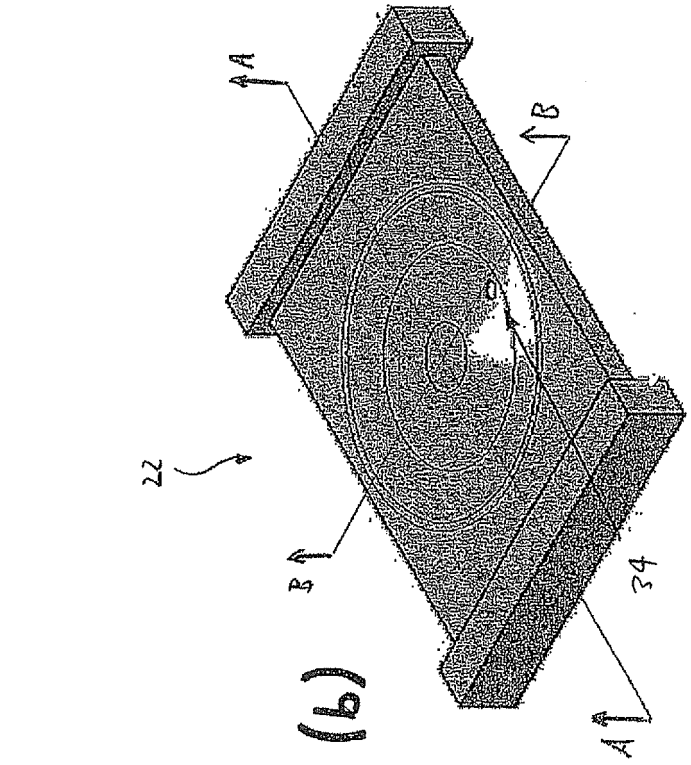

Fig. 8

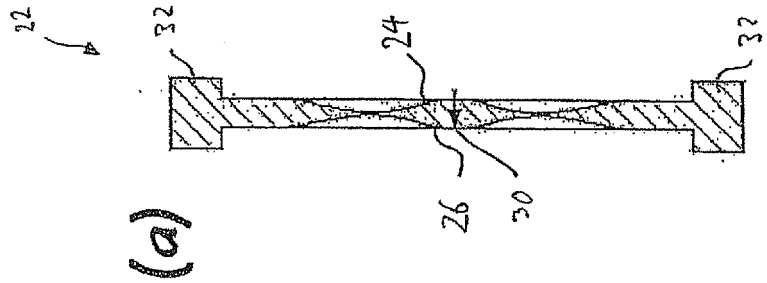

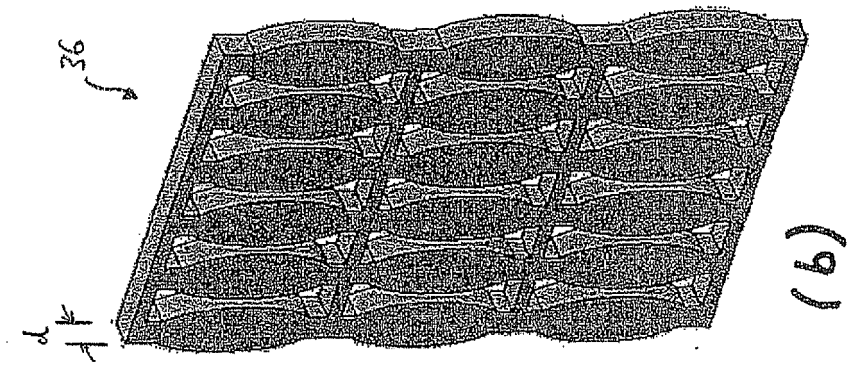

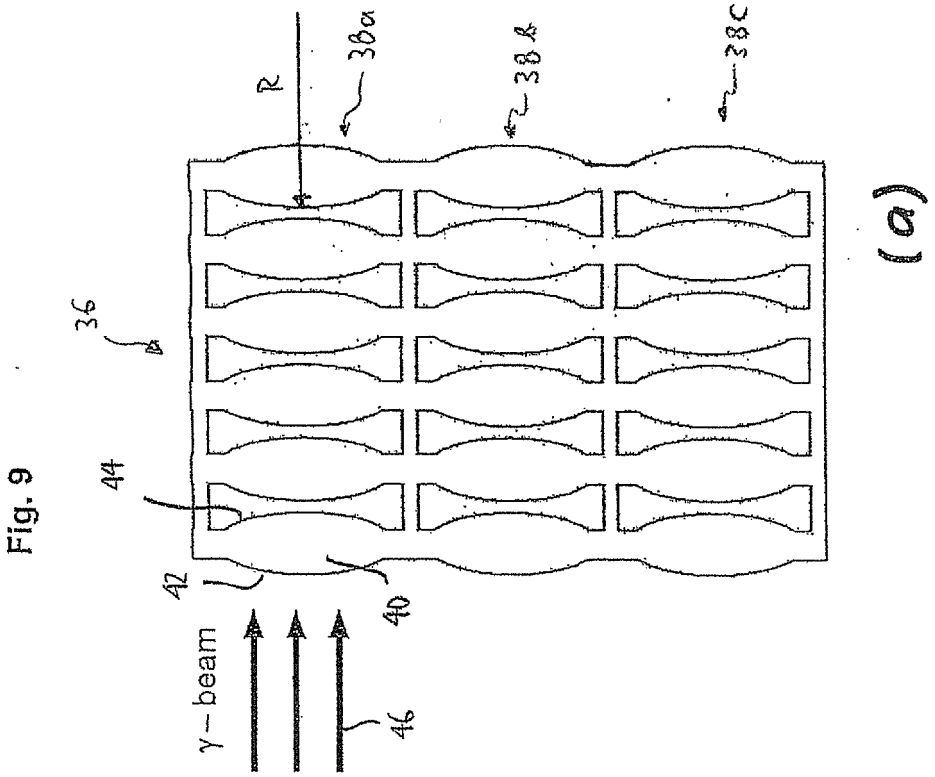

Fig. 9

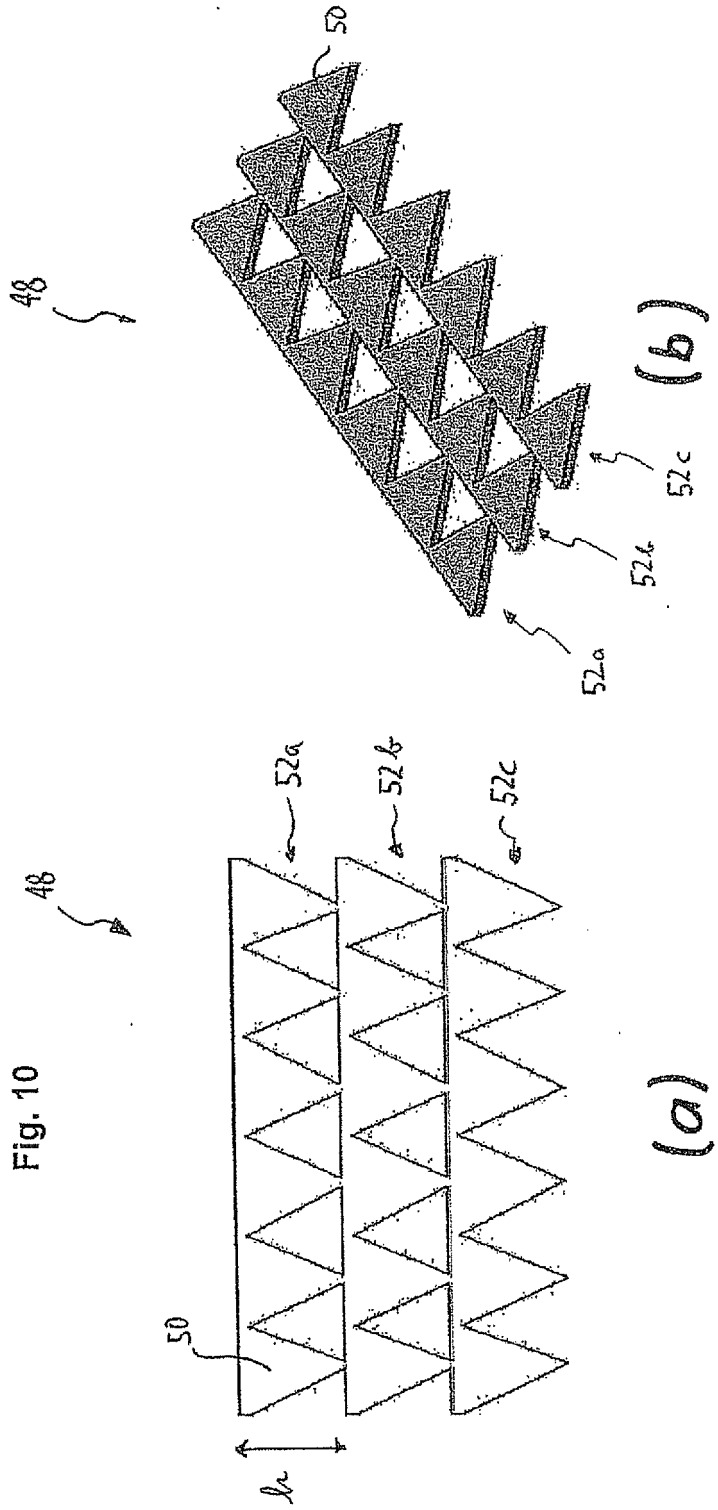

Fig. 10

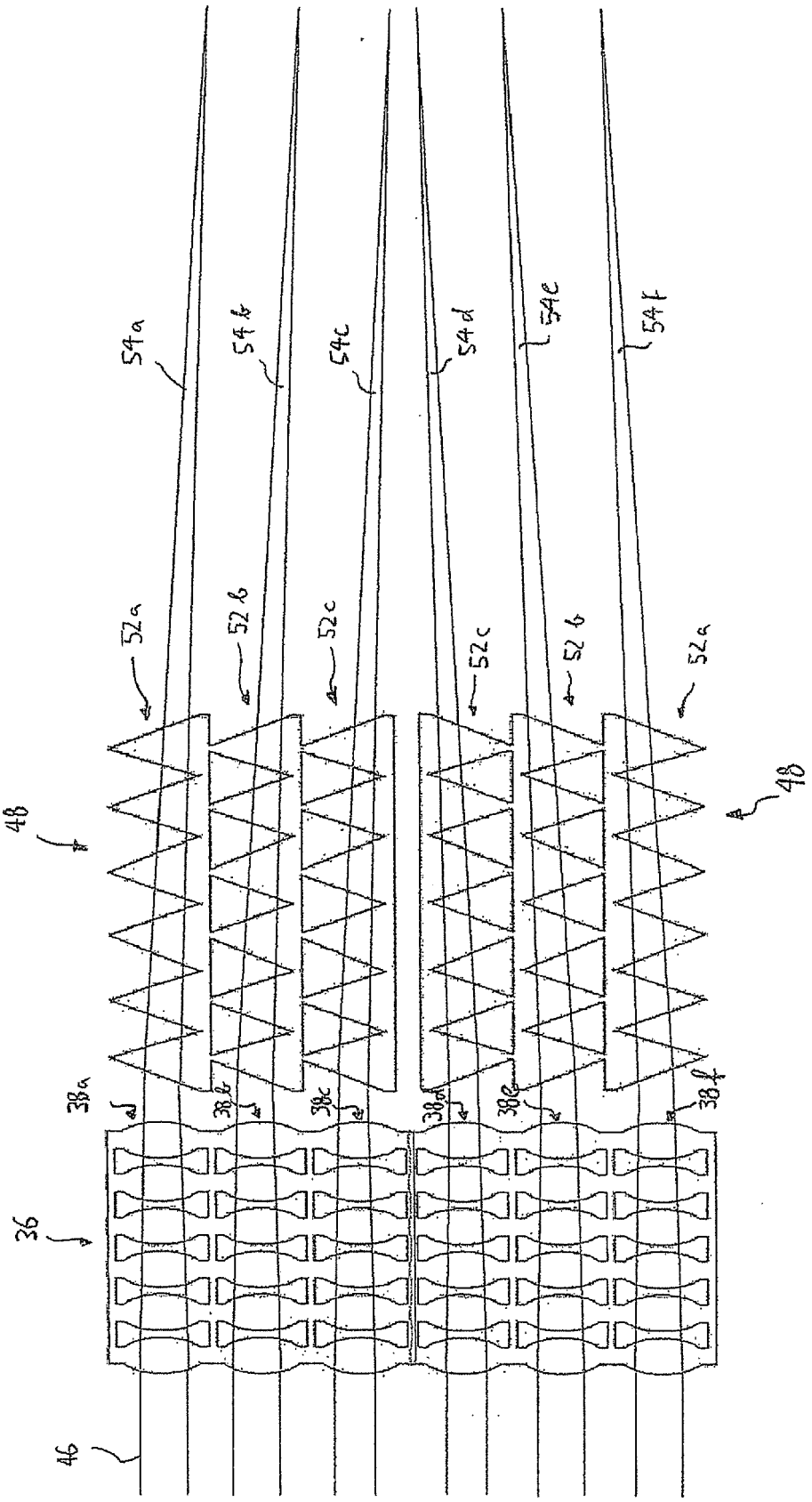
54a
54b
54c
54d
54e
54f
52a
52b
52c
52c
52b
52a
48
48
38a
38b
38c
38d
38e
38f
36
46

Fig. 11

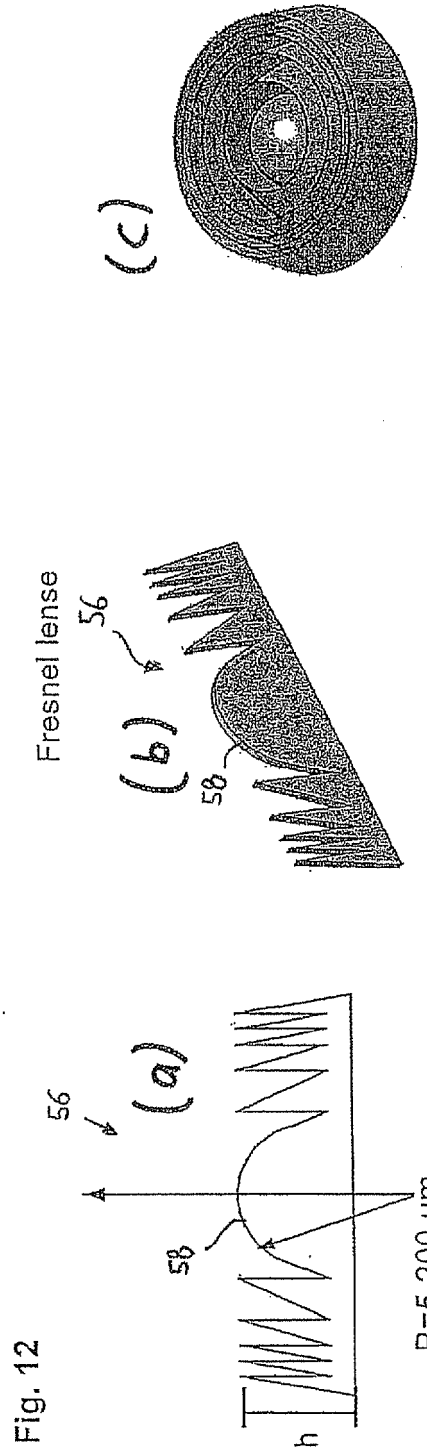
(a)
56
58
h
R=5-200 μm
Of convex ellipsoid
(b)
Fresnel lense
56
58
(c)

Fig. 12

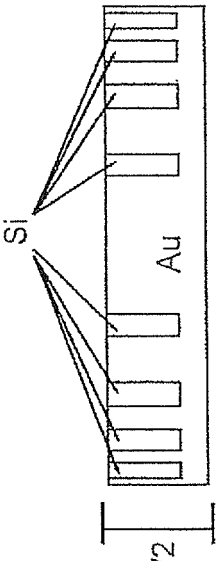
Si
Au
h/2

Fig. 13

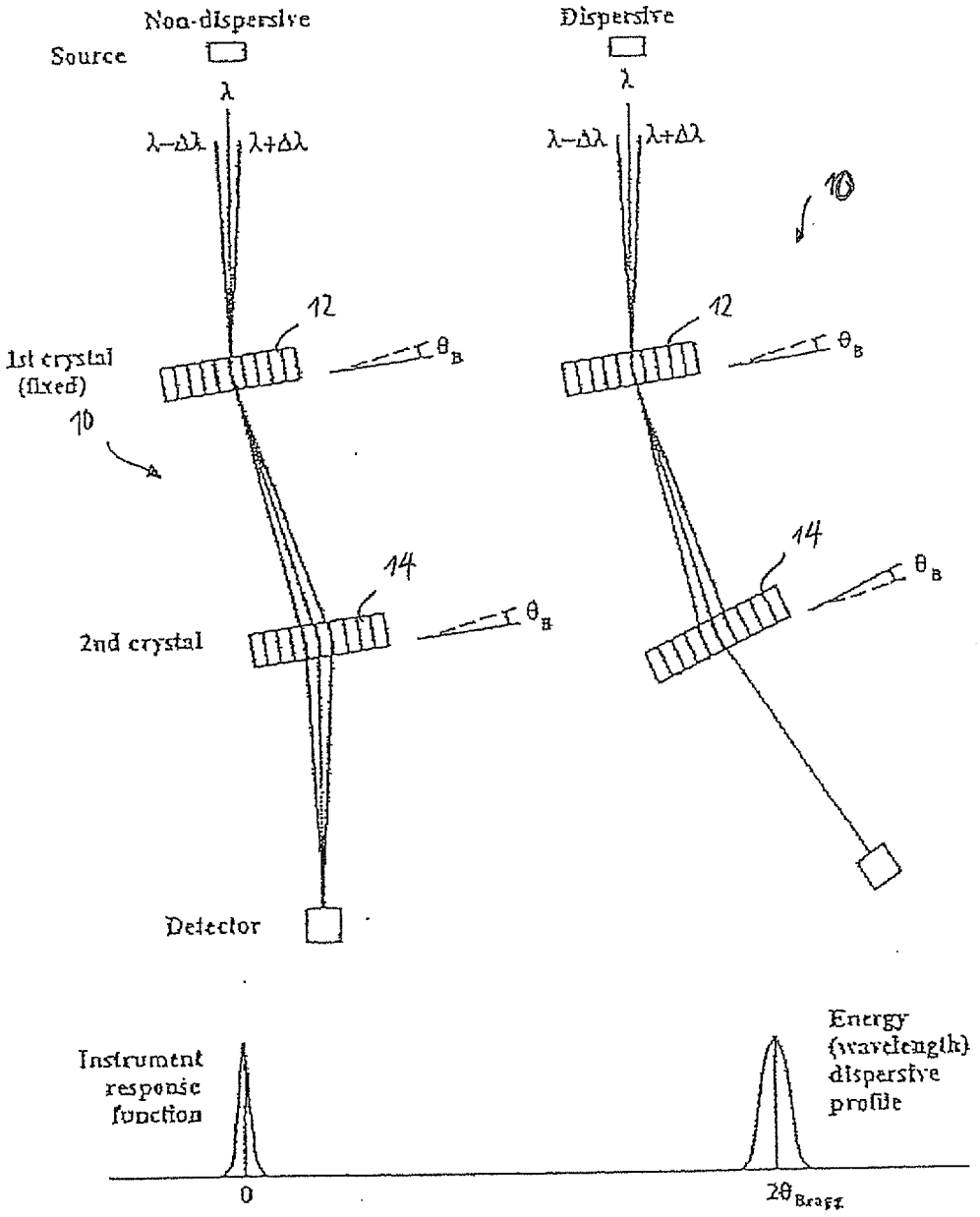
Non-dispersive
Source
λ
λ−Δλ
λ+Δλ
12
1st crystal
(fixed)
θB
10
14
2nd crystal
θB
Detector
Dispersive
λ
λ−Δλ
λ+Δλ
10
12
θB
14
θB
Instrument
response
function
0
Energy
(wavelength)
dispersive
profile
2θBragg

Fig. 14

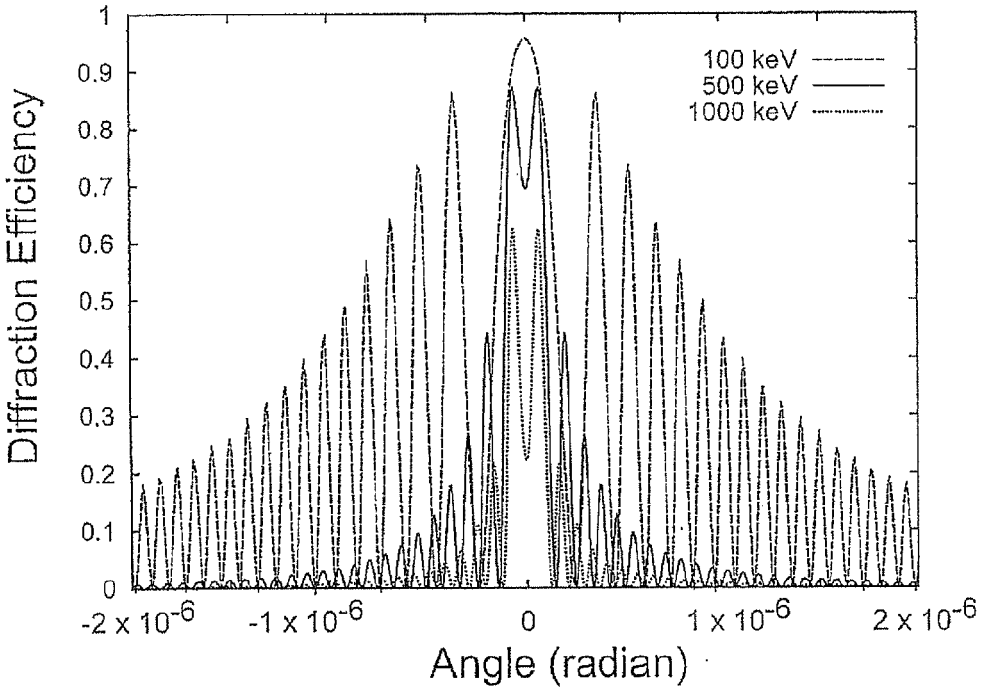
Diffraction Efficiency
1
0.9
0.8
0.7
0.6
0.5
0.4
0.3
0.2
0.1
0
100 keV
500 keV
1000 keV
-2 x 10-6
-1 x 10-6
0
1 x 10-6
2 x 10-6
Angle (radian)

Fig. 15

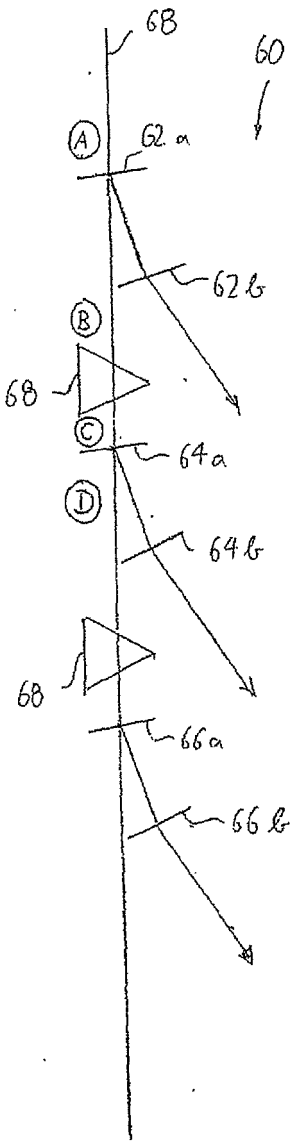
68
60
A
62a
62b
B
68
C
64a
D
64b
68
66a
66b

Fig. 16

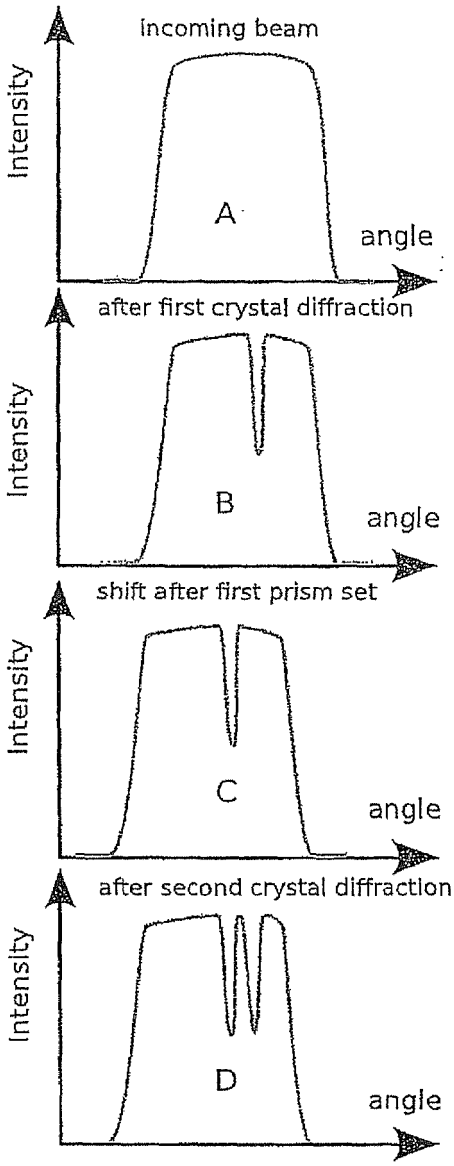
Incoming beam
Intensity
A
angle
after first crystal diffraction
Intensity
B
angle
shift after first prism set
Intensity
C
angle
after second crystal diffraction
Intensity
D
angle

Fig. 17

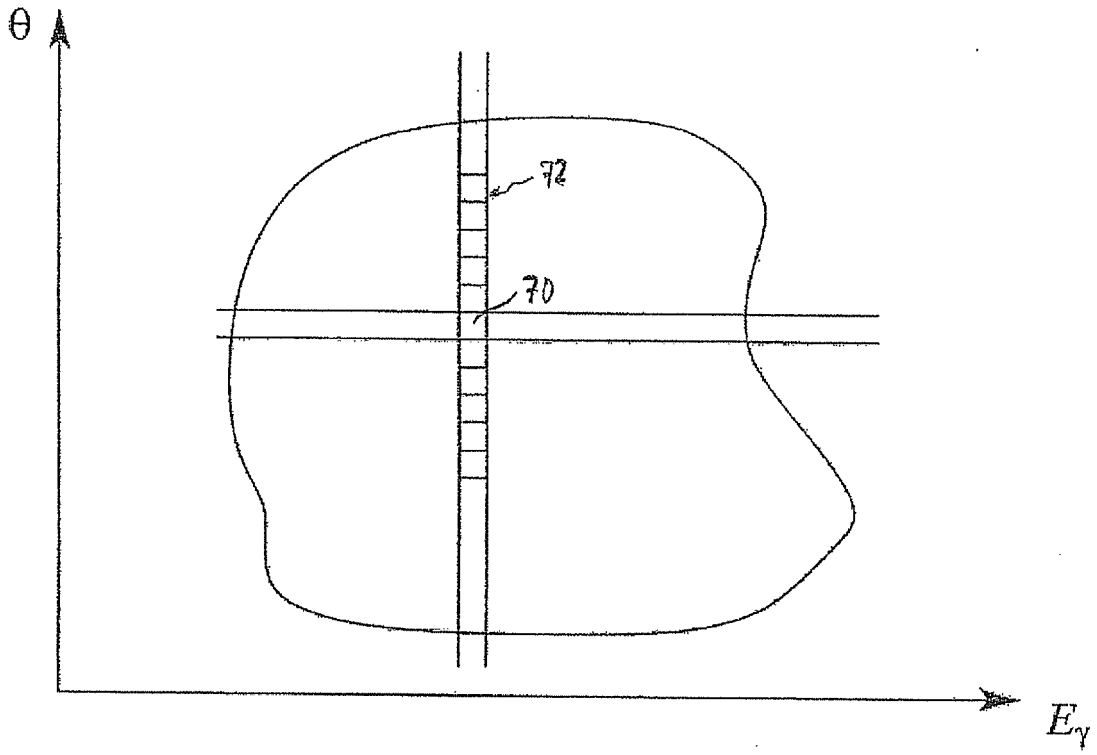

Fig. 18

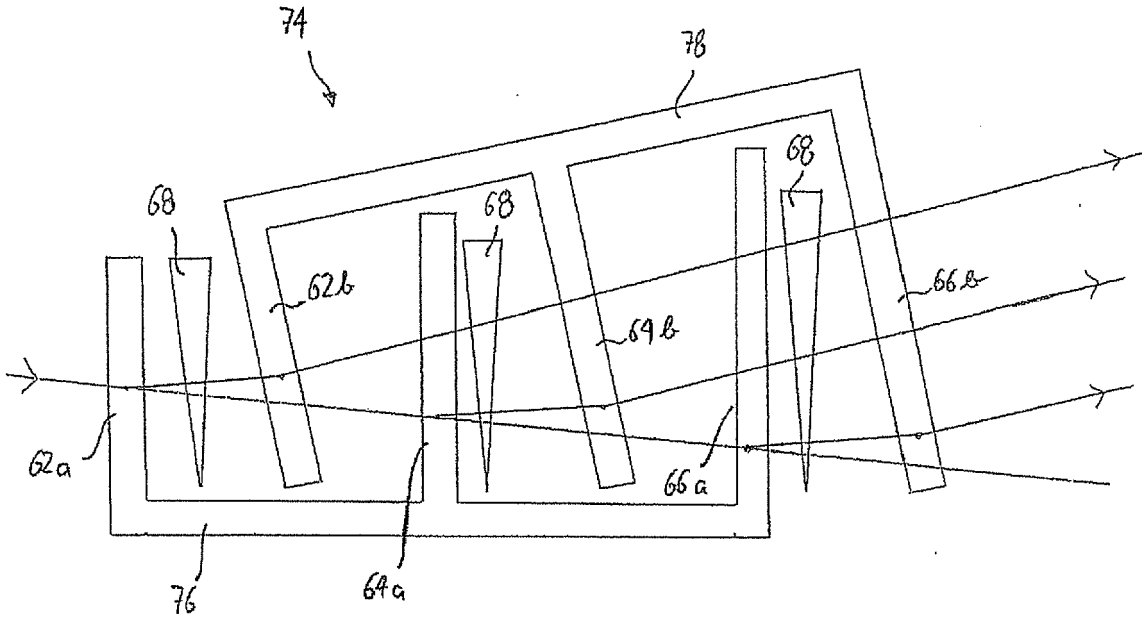

Fig. 19

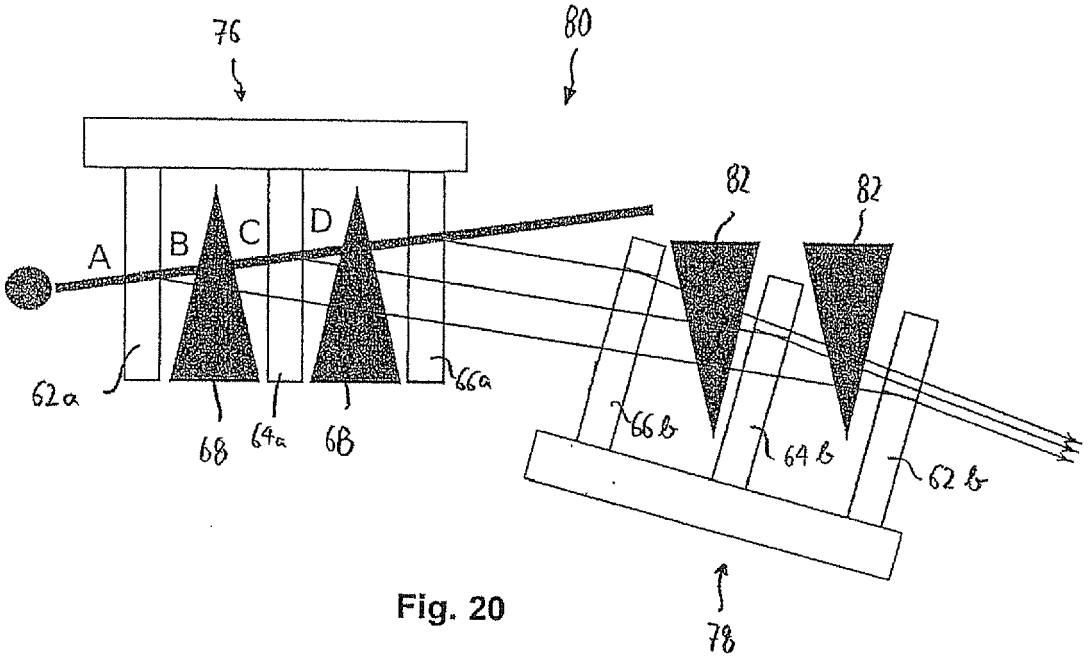

Fig. 20

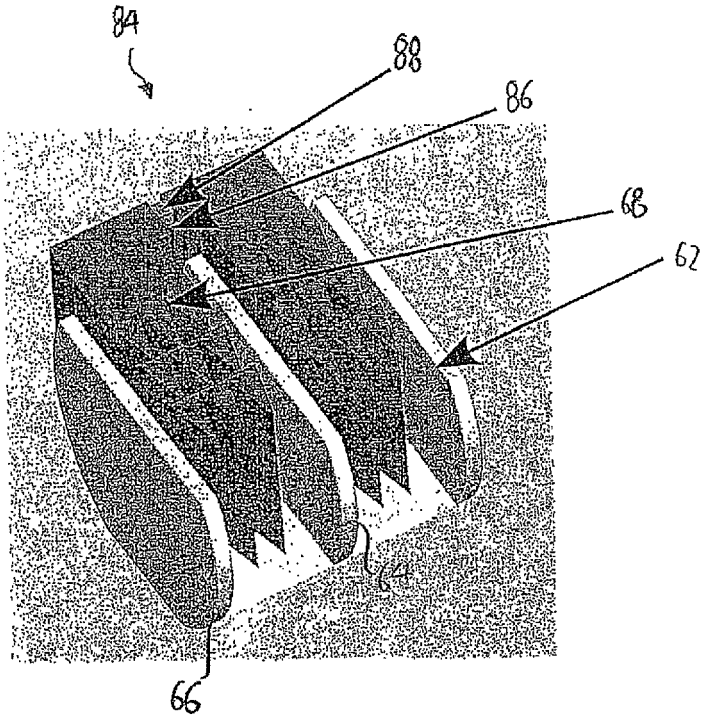

Fig. 21

Europäisches Patentamt
European Patent Office
Office européen des brevets

EUROPEAN SEARCH REPORT

Application Number
EP 11 19 5264

DOCUMENTS CONSIDERED TO BE RELEVANT

Category	Citation of document with indication, where appropriate, of relevant passages	Relevant to claim	CLASSIFICATION OF THE APPLICATION (IPC)
X	D. HABS ET AL: "Intense, brilliant micro [gamma]-beams in nuclear physics and applications", PROCEEDINGS OF SPIE, vol. 8075, 5 May 2011 (2011-05-05), page 807507, XP055049819, ISSN: 0277-786X, DOI: 10.1117/12.891512	1,2,5,6	INV. G21K1/06
A	* the whole document *	3,4, 8-10,14, 15	

X	A. Snigirev, I. Snigireva: "Hard X-Ray Microoptics" In: Alexei Erko, Mourad Idir, Thomas Krist, Alan G. Michette: "Modern Developments in X-Ray and Neutron Optics", 2008, Springer Berlin Heidelberg New York, XP002690461, ISBN: 978-3-540-74560-0 pages 260-279, * table 17.2 * * page 264 - page 276 *	1,7	
	-----		TECHNICAL FIELDS SEARCHED (IPC)
X	GERALD K. SKINNER: "Design and Imaging Performance of Achromatic Diffractive-Refractive X-Ray and Gamma-Ray Fresnel Lenses", APPLIED OPTICS, vol. 43, no. 25, 1 January 2004 (2004-01-01), page 4845, XP055049669, ISSN: 0003-6935, DOI: 10.1364/AO.43.004845 * page 4846; figure 1 * * page 4849; figure 5a *	10-13	G21K

	-/--		

The present search report has been drawn up for all claims

Place of search	Date of completion of the search	Examiner
Munich	23 January 2013	Giovanardi, Chiara

CATEGORY OF CITED DOCUMENTS

X : particularly relevant if taken alone
Y : particularly relevant if combined with another document of the same category
A : technological background
O : non-written disclosure
P : intermediate document

T : theory or principle underlying the invention
E : earlier patent document, but published on, or after the filing date
D : document cited in the application
L : document cited for other reasons

& : member of the same patent family, corresponding document

EPO FORM 1503 03.82 (P04C01)

Europäisches Patentamt
European Patent Office
Office européen des brevets

EUROPEAN SEARCH REPORT

Application Number
EP 11 19 5264

DOCUMENTS CONSIDERED TO BE RELEVANT

Category	Citation of document with indication, where appropriate, of relevant passages	Relevant to claim	CLASSIFICATION OF THE APPLICATION (IPC)
X	US 2010/296171 A1 (LEE SUSANNE MADELINE [US] ET AL) 25 November 2010 (2010-11-25) * figures 24,32,33,34 * * paragraphs [0002], [0003], [0052], [0073], [0077], [0078], [0080], [0081] * * paragraphs [0090], [0101], [0102] * -----	1	
A	DD 133 487 A1 (BOTHE HANS KARL; KOERNER GUENTHER) 3 January 1979 (1979-01-03) * page 1, lines 1-6 * * page 3, lines 5-27 * -----	8,9,14, 15	
A	TAKEYAMA A ET AL: "Computed tomography for reconstructing refractive index distribution using an X-ray shearing interferometer", SICE. PROCEEDINGS OF THE SICE ANNUAL CONFERENCE. INTERNATIONALSESSION PAPERS, TOKYO, JP, vol. 4, 7 August 2002 (2002-08-07), pages 2524-2526, XP008096633, * the whole document * -----	8,9,14, 15	TECHNICAL FIELDS SEARCHED (IPC)
A	US 2008/019482 A1 (YONEYAMA AKIO [JP] ET AL) 24 January 2008 (2008-01-24) * figures 10,12 * * paragraphs [0010], [0017], [0020], [0023], [0025], [0044], [0045] * * paragraphs [0054], [0085], [0086], [0089] * -----	8,9,14, 15	

The present search report has been drawn up for all claims

Place of search	Date of completion of the search	Examiner
Munich	23 January 2013	Giovanardi, Chiara

CATEGORY OF CITED DOCUMENTS

X : particularly relevant if taken alone
Y : particularly relevant if combined with another document of the same category
A : technological background
O : non-written disclosure
P : intermediate document

T : theory or principle underlying the invention
E : earlier patent document, but published on, or after the filing date
D : document cited in the application
L : document cited for other reasons

& : member of the same patent family, corresponding document

EPO FORM 1503 03.82 (P04C01)

ANNEX TO THE EUROPEAN SEARCH REPORT ON EUROPEAN PATENT APPLICATION NO. EP 11 19 5264

This annex lists the patent family members relating to the patent documents cited in the above-mentioned European search report. The members are as contained in the European Patent Office EDP file on
The European Patent Office is in no way liable for these particulars which are merely given for the purpose of information.

23-01-2013

Patent document cited in search report	Publication date	Patent family member(s)	Publication date
US 2010296171 A1	25-11-2010	EP 2433164 A2	28-03-2012
		JP 2012527649 A	08-11-2012
		US 2010296171 A1	25-11-2010
		WO 2010135024 A2	25-11-2010
DD 133487 A1	03-01-1979	NONE	
US 2008019482 A1	24-01-2008	JP 5041750 B2	03-10-2012
		JP 2008026098 A	07-02-2008
		US 2008019482 A1	24-01-2008

EPO FORM P0459

For more details about this annex : see Official Journal of the European Patent Office, No. 12/82

REFERENCES CITED IN THE DESCRIPTION

This list of references cited by the applicant is for the reader's convenience only. It does not form part of the European patent document. Even though great care has been taken in compiling the references, errors or omissions cannot be excluded and the EPO disclaims all liability in this regard.

Non-patent literature cited in the description

- **H.R. WELLER et al.** *Prog. Part. Nucl. Phys.,* 2009, vol. 62, 257 **[0004]**
- **E.G. KESSLER et al.** *Nucl Inst. Meth. A,* 2001, vol. 45 (7), 187 **[0065]**
- **R.L. MÖSSBAUER.** Recoilless Nuclear Resonance Absorption. *Ann. Rev. Nucl. Sci.,* 1962, vol. 12, 123 **[0078]**
- **R.L. MÖSSBAUER.** *Z.f. Physik,* 1958, vol. 151, 124 **[0078]**
- **H.A. BETHE ; F. ROHRLICH.** *Phys. Rev.,* 1952, vol. 86, 10 **[0079] [0082]**
- **F. ROHRLICH et al.** *Phys. Rev.,* 1952, vol. 86, 1 **[0079] [0082]**
- **H.A. BETHE et al.** *Proc. Roy. Soc. (London),* 1934, vol. 146, 83 **[0083]**
- **D.M PAGANIN.** Coherent X-Ray Optics. Oxford University Press, 2006 **[0088]**
- **E.G. KESSLER et al.** *Nucl Inst. Meth. A,* 2001, vol. 457, 187 **[0108]**
- **D. HABS et al.** *App. Phys. B,* 2011, vol. 103, 485 **[0136]**
- **C. HUGENSCHMIDT et al.** *Appl. Phys. B,* 2011 **[0137]**
- **C.G. SCHROER et al.** *Phys. Rev. Let.,* 2008, vol. 1001, 090801 **[0140]**
- **D.M. PAGANIN.** Coherent X-Ray Optics. Oxford University Press, 2006 **[0140]**